

1 Earliest infections predict the age distribution 2 of seasonal influenza A cases

3 Philip Arevalo¹, Huong Q. McLean², Edward A. Belongia², Sarah Cobey¹

4 For correspondence:

5 Philip Arevalo, parevalo@uchicago.edu

6 ¹Department of Ecology and Evolution, University of Chicago, Chicago, United States; ²
7 Center for Clinical Epidemiology and Population Health, Marshfield Clinic Research Institute,
8 Marshfield, United States

9 Abstract

10 Seasonal variation in the age distribution of influenza A cases suggests that factors other than age
11 shape susceptibility to infection. Here, we ask whether these differences can be explained in part by
12 protection conferred by childhood influenza infection, which has lasting impacts on immune responses
13 to influenza and protection against novel influenza A subtypes (phenomena known as original antigenic
14 sin and immune imprinting). Fitting a statistical model to 11 years of data from studies of influenza
15 vaccine effectiveness (VE) in Marshfield, Wisconsin, we find that primary infection appears to reduce
16 the risk of medically attended infection with that subtype throughout life and shapes the distribution of
17 seasonal influenza A cases. This effect is particularly strong for H1N1 (66% reduction in medically
18 attended H1N1 infection risk, CI 53-77%) compared to H3N2 (33% reduction in medically attended
19 H3N2 infection risk, CI 17-46%). Additionally, we find evidence that influenza VE varies with both age
20 and birth year, but not with the imprinting subtype per se. This suggests that VE may be sensitive to
21 particular exposure histories. The ability to predict age-specific risk might improve forecasting models
22 and vaccination strategies to combat seasonal influenza.

23 Introduction

24 Seasonal influenza is a serious public health concern, resulting in over 100,000 hospitalizations and
25 4,000 deaths per year in the United States despite extensive annual vaccination campaigns (Reed et al.
26 (2015)). The rapid evolution of the virus to escape preexisting immunity contributes to the relatively high
27 incidence of influenza, including in previously infected older children and adults. How susceptibility
28 arises and changes over time in the host population has been difficult to quantify.

29 A pathogen's rate of antigenic evolution should affect the mean age of the hosts it infects, and
30 differences in the rate of antigenic evolution have been proposed to explain differences in the age
31 distributions of the two subtypes of influenza A. Compared to H3N2, H1N1 disproportionately infects
32 children (Caini et al. (2018); Khiabani et al. (2009)). It also evolves antigenically more slowly
33 (Bedford et al. (2015)). Thus, compared to H3N2, H1N1 is slower to escape immunity in individuals
34 who have experienced prior infection (namely older children and adults), making them less susceptible
35 to reinfection (Bedford et al. (2015); Beauté et al. (2015); Caini et al. (2018); Khiabani et al. (2009)).

36 H3N2, in contrast, exhibits well known changes in antigenic phenotype that are expected to drive cases
37 toward adults (Smith et al. (2004); Cobey and Koelle (2008)). Under this simple model, hosts previously
38 infected with a subtype face equal risk of reinfection (on challenge) with an antigenic variant of that
39 subtype.

40 The age distributions of influenza infections in exceptional circumstances—pandemics and spillovers
41 of avian influenza—have shown unexpected variation that suggests potentially complex effects of prior
42 infection. Excess mortality in some adult cohorts during the 1918 and 2009 H1N1 pandemics has been
43 linked to childhood infection with particular subtypes (Gagnon et al. (2013); Worobey et al. (2014);
44 Gagnon et al. (2018)). Similarly, the subtypes circulating in childhood predict individuals' susceptibility
45 to severe zoonotic infections with avian H5N1 and H7N9, regardless of later exposure to other seasonal
46 subtypes (Gostic et al. (2016); Budd et al. (2019)). These patterns suggest that early influenza infections,
47 and not prior infection per se, strongly shape susceptibility.

48 Early infections might also affect the protection conferred by influenza vaccination. Foundational
49 work on the theory of original antigenic sin demonstrated that an individual's immune response to
50 influenza vaccination is biased toward antigens similar to those encountered in childhood (Davenport
51 and Hennessy (1956, 1957)). This phenomenon has been suggested to explain an unexpected decrease
52 in vaccine effectiveness (VE) in the middle-aged in the 2015-2016 influenza season (Skowronski et al.
53 (2017b); Flannery et al. (2018)). More generally, it has been hypothesized that biases in immune memory
54 can arise from both past infections and vaccinations, leading to variation in vaccine effectiveness that is
55 sensitive to the precise history of exposures (Smith et al. (1999); Skowronski et al. (2017a)).

56 To measure the effect of early exposures on infection risk and VE, we fitted statistical models
57 to 3493 influenza cases identified through seasonal studies of influenza VE from the 2007-2008 to
58 2017-2018 seasons in Marshfield, Wisconsin (Belongia et al. (2009, 2011); Griffin et al. (2011); Treanor
59 et al. (2012); Ohmit et al. (2014); McLean et al. (2014b); Gaglani et al. (2016); Zimmerman et al. (2016);
60 Jackson et al. (2017); Flannery et al. (2018)). Each season, individuals in a defined community cohort
61 were recruited and tested for influenza when seeking outpatient care for acute respiratory infection.
62 Eligibility was restricted to individuals >6 months of age living near Marshfield who received routine
63 care from the Marshfield Clinic. After obtaining informed consent, a mid-turbinate swab was obtained
64 for influenza detection. RT-PCR was performed using CDC primers and probes to identify influenza
65 cases, including type and subtype.

66 We sought to explain the variation in the age distribution of these cases by subtype and over time.
67 Our model predicted the relative number of cases of influenza in each birth year each season as a function
68 of the age structure of the population, age-specific differences in the risk of medically attended influenza
69 A infection, early influenza infection, and vaccination. Despite the extensive antigenic evolution in both
70 subtypes over the study period, we found strong evidence of protection from the subtype to which a
71 birth cohort was likely first infected (the imprinting subtype) and variation in VE by birth cohort.

72 Results

73 The age distribution of cases varies significantly between seasons and subtypes

74 We examined the age distribution of cases of the dominant (most common) subtype in each season
75 between 2007-2008 and 2017-2018 among enrolled patients. We excluded the subdominant subtype in
76 each season due to concerns that short-term interference between the subtypes (Laurie et al. (2015);
77 Goldstein et al. (2011)) would disproportionately affect the age distribution of the rarer subtype.
78 Differences between all pairs of seasons were evaluated by the G-test of independence and corrected
79 for multiple tests (Materials and Methods: "Calculating differences in the age distribution between
80 seasons").

81 The age distribution of cases varies significantly between subtypes. The relative burden of cases is
82 consistently higher in people over 65 years old during H3N2-dominated seasons compared to H1N1-
83 dominated seasons (Figure 1), and nearly all H1N1-dominated seasons have significantly different age
84 distributions from all H3N2-dominated seasons (Figure 1-Supplement 1, off-diagonal quadrants).

85 The age distribution also varies significantly within subtypes over time (Figure 1-Supplement 1,
86 diagonal quadrants). The seven H3N2-dominated seasons display three types of age distributions
87 (Figure 1-Supplement 1, white patches in upper left-hand quadrant), and two correspond to major
88 antigenic clusters (2007-2008 Fonville et al. (2015), 2010-2012 Ann et al. (2012)). These differences
89 sometimes coincide with significant shifts in the age distribution between seasons. For instance, the
90 highest fraction of H3N2 cases occurs in 20-29 year olds in the 2007-2008 season, but this age group
91 has the lowest fraction of cases in the next H3N2-dominated season (2010-2011, Figure 1C). In H1N1,
92 the shift from seasonal to pandemic strains is associated with a significant change in the age distribution
93 (Figure 1-Supplement 1, lower right-hand quadrant). The high fraction of cases among 40-64 year-olds
94 in the 2013-2014 season (Figure 1B) has been attributed to the emergence of strains to which this group
95 was especially susceptible (Linderman et al. (2014); Petrie et al. (2016)).

96 We found further evidence that age groups differed in their susceptibility across seasons by examining
97 the relative risk of infection during the first versus second half of each epidemic period (Materials
98 and Methods: "Calculating relative risk"). Because more susceptible populations experience higher
99 attack rates, individuals in these populations should be infected disproportionately early rather than late
100 in an epidemic (Worby et al. (2015)). We confirmed that an age group's relative risk of infection in
101 the first versus the second half of each epidemic correlates with the total fraction of cases in that age
102 group that season (Spearman's $\rho=0.41$, $p=0.001$, Figure 1-Supplement 2A). This trend is significant
103 for H1N1 (Spearman's $\rho=0.47$, $p=0.02$, Figure 1-Supplement 2A) and H3N2 seasons separately
104 (Spearman's $\rho=0.35$, $p=0.05$, Figure 1-Supplement 2A). The positive correlation in all seasons is robust
105 to undersampling of cases at the start or end of specific seasons (Materials and Methods: "Sensitivity
106 to sampling effort", Figure 1-Supplement 2B). This provides supporting evidence that the different
107 numbers of cases in each age group reflect underlying differences in susceptibility.

108 Just as the age distribution of cases varies over time, the age groups with the highest relative risk of
109 infection, and by implication susceptibility, also change across seasons. For instance, 5-17 year olds
110 had the highest relative risk of early infection in the 2008-2009 season, whereas 50-64 year-olds had
111 the highest relative risk in the 2013-2014 season (Figure 1-Supplement 3). Relative risk in Marshfield

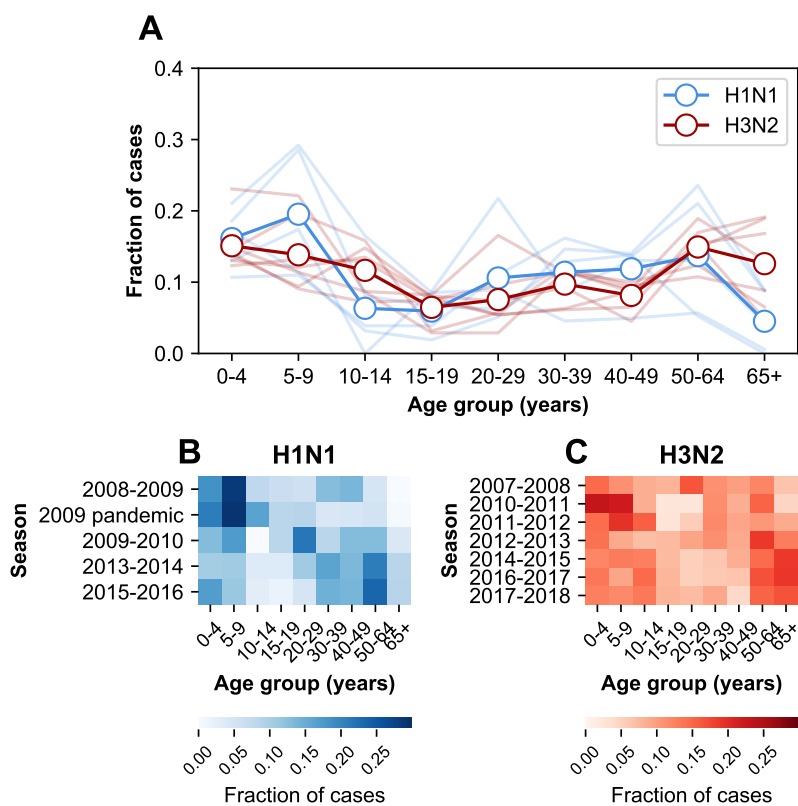


Figure 1. **A.** The age distributions of cases from the 2007-2008 through the 2017-2018 influenza seasons in Marshfield. Dark lines with open circles indicate the average fraction of cases in each age group. Lighter-colored lines show the age distribution for individual seasons. **B.** The age distribution of cases in H1N1-dominated seasons. **C.** The age distribution of cases in H3N2-dominated seasons.

112 is considerably more variable than national estimates, which showed that 5-17 year-olds had the highest
 113 relative risk in all but one season from the 2009 pandemic to 2013-2014 (Worby et al. (2015)). These
 114 differences may be due in part to the fact that our measurements of relative risk used outpatient visits,
 115 whereas the national estimates used hospitalizations.

116 Taken together, these findings suggest that the risk of influenza infection is not a simple function of
 117 age alone. Other factors, such as past influenza infections and vaccination, might explain the changing
 118 age distributions of cases in time.

119 **Imprinting probabilities of age groups change over time**

120 We hypothesized that variation in the age distribution of cases could be explained by the aging of birth
 121 cohorts with similar early exposure histories. This would cause the early exposure history of an age
 122 group to change in time. To calculate the probability that an individual in a particular age group had
 123 their first influenza A infection with a particular subtype, we adapted the approach from Gostic et al.
 124 (2016). Briefly, we calculated the probability that an individual born in a specific year had their first
 125 infection with H1N1, H2N2, or H3N2 using data on relative epidemic sizes and the frequencies of
 126 circulating subtypes (Figure 2-Supplement 1).

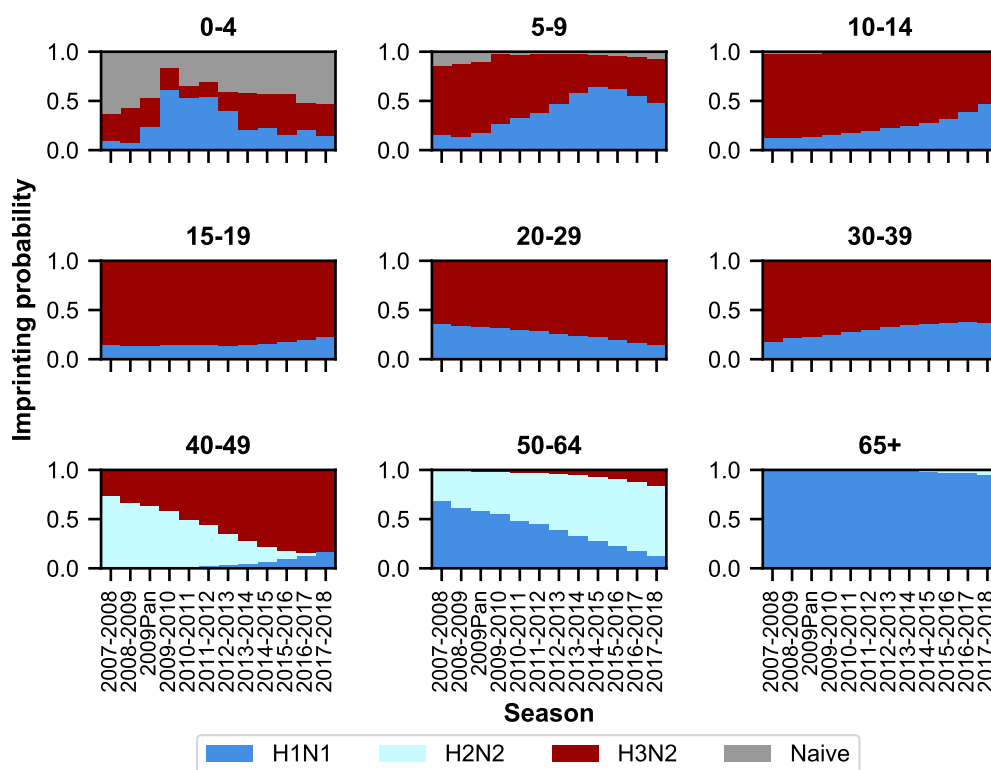


Figure 2. The imprinting probabilities of age groups change over time. Each panel shows the imprinting probabilities of an age group from the 2007-2008 season through the 2017-2018 season. The color of each bar corresponds to the imprinting subtype or naive individuals, who have not yet been infected.

127 As expected, age groups' early exposures are not static and change over time (Figure 2). Older people
 128 nonetheless tend to be imprinted to H1N1 or H2N2, whereas younger people have higher probabilities
 129 of imprinting to H3N2. The effects of the 2009 H1N1 pandemic are evident in the three youngest age
 130 groups as a transient increase (from 2009 to approximately 2013) in their H1N1 imprinting probability.

131 Modeling approach

132 We fitted a set of models to estimate the effects of demography, age, imprinting, and vaccination on the
 133 age distribution of influenza cases. The number of observed cases in influenza season t among people
 134 born in year y is proportional to a combination of these factors:

- 135 1. *Demography.* The age distribution of our study cohort is not static over the study period. All
 136 models adjust for the changing fractions of the population in each birth cohort and season
 137 (Figure 3-Supplement 1, Materials and Methods: "Demography").
- 138 2. *Age-specific effects.* We consider that age itself may be associated with differences in influenza A
 139 infection risk stemming from differences in susceptibility and/or rates of contact with infectious
 140 people. Additionally, we expect that age groups may intrinsically differ in their healthcare-seeking
 141 behaviors. These factors are inseparable in our data, and all models represent their combined
 142 effects with a static age-specific parameter shared by both subtypes that describes the risk of
 143 age-specific medically attended influenza A infection (Materials and Methods: "Age-specific

144 factors"). Thus, we assume no intrinsic differences in the age-specific virulence of the two
145 subtypes. These age-specific parameters are fitted. We also adjust for other potential sources of
146 age-specific bias, including age-specific differences in study approachment and enrollment rates
147 (Materials and Methods: "Age-specific factors").

148 3. *Imprinting*. We tested several hypotheses of how primary exposures could affect the risk of
149 infection with H1N1 and H3N2. In each version, we estimated fractional reductions in risk to
150 H1N1 and H3N2 due to primary (i.e., imprinting) exposure to the same type:

151 • Subtype-specific imprinting: Influenza has two main antigens, hemagglutinin (HA) and
152 neuraminidase (NA). Imprinting could in theory derive from responses to either or both
153 antigens. Because H1N1 is the only seasonal subtype of influenza with N1, we cannot
154 separate the effects of initial N1 exposure from initial H1 exposure. However, since N2
155 appears in both H3N2 and H2N2 viruses, we can estimate protection against H3N2 infection
156 from initial N2 exposure separately from protection from initial H3 exposure (Materials
157 and Methods: "HA subtype imprinting" and "N2 imprinting").

158 • Group-level imprinting: Influenza A viruses fall into two groups (I and II) corresponding to
159 the two phylogenetic clades of HA. Gostic et al. (2016) found that primary infection by a
160 virus belonging to one group protected against severe infection by another subtype in the
161 same group. If group-level imprinting were influential, we would see primary infection
162 with H2N2 conferring protection against H1N1, another group I virus, as well as H1N1
163 protecting against H1N1 and H3N2 against H3N2. We considered a separate class of models
164 that assumes group-level protection instead of subtype-specific protection (Materials and
165 Methods: "HA group imprinting").

166 4. *Vaccination*. Approximately 45% of the population of Marshfield is vaccinated against influenza
167 each year. We estimated cases in vaccinated and unvaccinated individuals of each birth year
168 separately. Naively, we expect that vaccinated individuals should seek medical attention for
169 acute respiratory infection (ARI) proportionally to the fraction of their cohort vaccinated that
170 season. However, vaccinated individuals may seek medical attention for ARI more frequently
171 than expected due to positive associations between the decision to vaccinate, healthcare-seeking
172 behavior, and underlying medical conditions (Jackson et al. (2005a,b); Belongia et al. (2009)). We
173 attempted to adjust for this by calculating the fraction of vaccinated people among those who had
174 a medically attended acute respiratory infection (MAARI) and tested negative for influenza (i.e.,
175 the test-negative controls, Materials and Methods: "Vaccination"). We find that this correlates
176 with but exceeds vaccination coverage for most age groups, suggesting vaccinated individuals are
177 overrepresented among cases for reasons unrelated to influenza (Figure 3-Supplement 2). We also
178 assume that vaccination is not perfectly effective, defining VE as the fractional reduction in cases
179 expected in vaccinated compared to unvaccinated individuals after controlling for the effects
180 described above. We estimated subtype-specific VE under five scenarios: (i) constant across age
181 groups and seasons; (ii) season-specific and constant across age groups; (iii) age-specific and
182 constant across seasons; (iv) imprinting-specific; and (v) birth-cohort-specific. We assumed that
183 vaccination affects risk only in the current season, i.e., there are no residual effects from prior

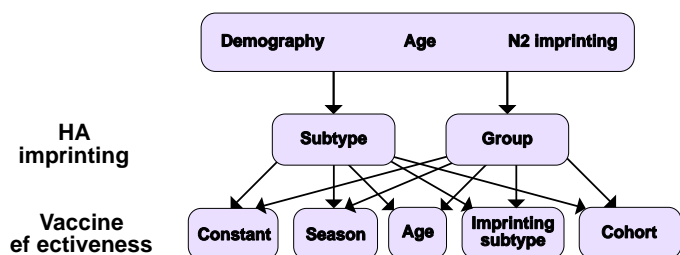


Figure 3. All models include demography, age effects, and the option of N2 imprinting. Ten different models result from considering different combinations of HA imprinting and VE.

184 vaccination (Materials and Methods: "Vaccination").

185 With these considerations, we evaluated the models by maximum likelihood and compared their
186 performance using the corrected Akaike information criterion (cAIC, Figure 3).

187 **Age-specific differences in medically attended influenza A infection risk affect epidemic** 188 **patterns**

189 As expected, the cases reveal age-specific differences in the risk of medically attended influenza A
190 infection. (Figure 4; Figure 4-Supplement 1; Appendix 1 Table 1). The risk of medically attended
191 influenza A infection is roughly threefold higher among children less than four years old compared
192 to adults 20-29 years old, after adjusting for other effects (Figure 4). This decline in risk with age is
193 consistent with findings that attack rates decrease with age (Monto et al. (1985); Bodewes et al. (2011);
194 Wu et al. (2010, 2017); Huang et al. (2019)). Additionally, rates of healthcare-seeking behavior have
195 been shown to decline with age before rising in adults over 65 years old (Biggerstaff et al. (2014);
196 Brooks-Pollock et al. (2011); Van Cauteran et al. (2012)), consistent with our results. Finally, the
197 increased risk of medically attended influenza A infection among people ≥ 65 years old relative to
198 other adults may be related to the increasing prevalence of high-risk medical conditions with age
199 (Figure 4-Supplement 2).

200 **Initial infection confers long-lasting, subtype-specific protection against future infection**

201 Our best-fitting model supports subtype-specific imprinting for H1N1 and H3N2 (Figure 5, top row;
202 Appendix 1 Table 1). The risk of future medically attended infection by H1N1 is reduced by 66% (95% CI
203 53-77%) in people imprinted to H1N1, whereas the risk of future medically attended infection by H3N2
204 is reduced by 33% (95% CI 17-46%) in people imprinted to H3N2. We found no evidence of a protective
205 effect from imprinting to N2 (0%, 95% CI 0-7%). Our estimates of imprinting protection are insensitive
206 to our choice of age groups for medically attended influenza A infection risk and VE (Appendix
207 1 Table 3) as well as undersampling of influenza cases in some seasons (Figure 5-Supplement 1,
208 Figure 5-Supplement 2, Materials and Methods, "Sensitivity to sampling effort").

209 We also tested whether vaccination is a plausible mechanism of imprinting (Figure 5-Supplement 3,
210 Materials and Methods, "Calculating imprinting probabilities") and found that primary exposure via
211 vaccination provided similar protection as imprinting from primary infection (100% of the effect

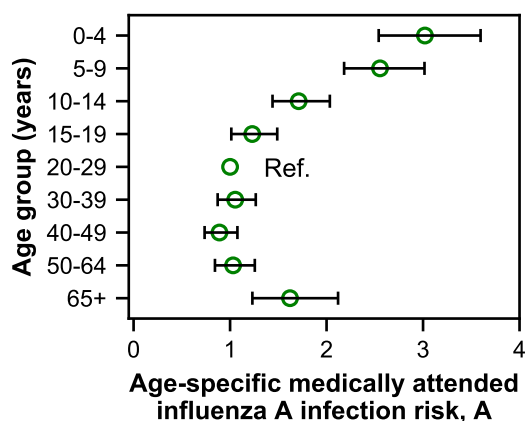


Figure 4. Open circles represent the maximum likelihood estimates of parameters describing age-specific differences in medically attended influenza A infection risk. Lines show the 95% confidence interval.

212 of primary infection, 95% CI 74-100%, Figure 5-Supplement 4, Materials and Methods, "Vaccine
213 imprinting"). However, the estimated protection could be confounded with residual protection from
214 prior season vaccination (Ohmit et al. (2014); McLean et al. (2014a,b)) which the model excludes.

215 In theory, the protective effects of imprinting that we measured could be influenced by cross-
216 protection rather than the impact of first infection per se. Because first infections are also recent
217 infections in children, we reasoned that the observed imprinting effects might arise from confounding
218 with recent infections in these ages. When we excluded the youngest age groups, our estimates of
219 H1N1 imprinting protection decreased while H3N2 imprinting protection increased (Figure 5, second
220 row). However, initial infection by H1N1 was still more protective than initial infection by H3N2, both
221 imprinting effects remained significantly positive, and there was no significant change in the values of
222 other estimated parameters (Appendix 1 Table 1 and Table 2).

223 We expect that confounding with recent infection should also manifest in the difference between the
224 observed and estimated number of cases (i.e., the excess cases, Materials and Methods: "Calculating
225 excess cases"), since our model does not take prior season infections into account when estimating cases
226 for the current season. More infections within a population in one season should reduce susceptibility
227 in that population at the start of the next season. We thus expect that a large number of excess cases
228 in one season will be followed by a small number of excess cases in the next season with the same
229 dominant subtype (i.e., a negative correlation). Instead, we observed that excess cases for each birth
230 cohort have a weak positive correlation from season to season, suggesting that immunity from recent
231 infections is not a primary driver of variation in the age distribution of cases (Figure 5-Supplement 5).

232 Since older adults have the highest probability of primary infection with H1N1, we also reasoned
233 that older adults might disproportionately drive the strong protection from H1N1 imprinting we observe.
234 People born before 1947 were likely exposed to H1N1 strains that are antigenically similar to the
235 post-pandemic H1N1 strains that comprise most of our H1N1 infection data (Manicassamy et al. (2010);
236 O'Donnell et al. (2012)), creating the possibility that strain-specific cross-immunity drives the pattern
237 we attribute to subtype-specific imprinting. Excluding the oldest adults, however, does not significantly

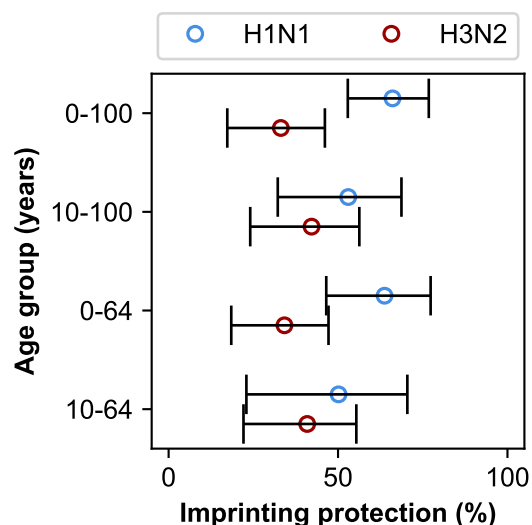


Figure 5. Imprinting is more protective against H1N1 infection than H3N2 infection. Open circles represent the maximum likelihood estimates of imprinting parameters from the best-fitting model for the indicated age group. Black lines show 95% confidence intervals.

238 change our estimates of imprinting protection or other parameters (Figure 5, third row, Appendix 1
239 Table 1, Table 2). When we exclude both the youngest and oldest age groups, initial infections by H1N1
240 and H3N2 have similar protective effects (Figure 5, bottom row). This suggests that the combined effects
241 of cross-protection in both the youngest and oldest individuals contribute to the signal of imprinting
242 protection we observe, but they are not its sole drivers.

243 **VE varies by birth cohort in older children and adults**

244 The best-fitting model includes age-specific VE (Figure 4-Supplement 1, Appendix 1 Table 2). While
245 serological responses to influenza vaccination are weakest in the young (Englund et al. (2005); Neuzil
246 et al. (2006)) and old (Lee et al. (2018); DiazGranados et al. (2014)), it is unclear what age-related
247 factors would drive variation in VE in other age groups. We hypothesized that VE in these ages is
248 specific to exposure history, which correlates with birth year, rather than age.

249 To test this hypothesis, we fitted a model with birth-cohort-specific VE to data excluding either
250 children <10 years old or adults ≥ 65 years old. We chose birth cohorts that corresponded to the
251 age groups of the original model in 2017-2018 (Materials and Methods: "Vaccination"), keeping the
252 number of parameters the same (e.g., VE in the 20-29 age group became VE in the 1988-1997 birth year
253 cohort). We find that age-specific VE still outperforms all other models after we exclude the oldest age
254 group (≥ 65 years old). In contrast, birth-cohort-specific VE performs better when we exclude children
255 <10 years old (Figure 6-Supplement 1). Estimates of imprinting protection and age-specific risk of
256 medically attended influenza in the birth-cohort-specific VE models are not significantly different from
257 estimates from the best-fitting model fitted to all ages (Appendix 1 Table 1). Taken together, these
258 results suggest that birth-cohort-specific VE best explains the case distribution in older children and
259 adults, who have likely experienced their first influenza infection, whereas age-specific VE best explains

260 cases in younger children, who have less influenza exposure.

261 VE differs between birth cohorts that have similar imprinting by subtype (Figure 6, Appendix
262 1 Table 4), suggesting that specific infection history (beyond imprinting subtype) is important. For
263 example, the 1968-1977 and 1988-1997 cohorts have similar probabilities of primary exposure to H1N1
264 and H3N2, but they differ substantially in their VE to both subtypes (Figure 6). The 1988-1997 and
265 1998-2002 cohorts also have similar probabilities of primary exposure to each subtype and have similar
266 H1N1 VEs, but have significantly different H3N2 VEs (Figure 6). Antigenic differences within each
267 subtype might explain this variation.

268 Our results support the idea that biases in immune memory from early exposures (i.e., original
269 antigenic sin; Davenport and Hennessy (1957); Francis (1960); Groth and Webster (1966)) influence
270 VE. The model with birth-cohort-specific VE better estimates cases among vaccinated 50-64 year-olds
271 (born 1953-1967) in the 2015-2016 season than the model with age-specific VE (Figure 6-Supplement 2,
272 Materials and Methods: "Calculating excess cases"). Reduced VE in this age group has been attributed
273 to the exacerbation of antigenic mismatch by the vaccine in adults whose antibody responses were
274 focused on a non-protective site (Skowronski et al. (2017b); Flannery et al. (2018)). The improved
275 performance of birth-cohort-specific VE relative to age-specific VE suggests other seasons and age
276 groups where original antigenic sin might have influenced VE, such as 20-29 year-olds in the 2007-2008
277 influenza season.

278 **Discrepancies partly explained by antigenic evolution**

279 The best-fitting model accurately reproduces the age distributions of vaccinated and unvaccinated cases
280 of each subtype, aggregated across seasons (Figure 7A). The only exception is that it underestimates
281 H1N1 cases in unvaccinated 5-9 year-olds. By examining the differences between predicted and
282 observed cases for each season, we see that this is largely driven by infection during the 2009 H1N1
283 pandemic (Figure 7B). Such a large antigenic change may have negated any protection from previous
284 infection in 5-9 year-olds and made them particularly susceptible to pandemic infection.

285 The model underestimates cases in unvaccinated individuals >30 years old in the 2013-2014 season.
286 This is further evidence that subtype-specific imprinting cannot explain all age variation. As mentioned
287 before, this season provided one of the first examples that original antigenic sin could affect protection:
288 middle-aged adults had been targeting a familiar site on the pandemic strain that then mutated; other age
289 groups were effectively blind to these changes, owing to their different exposure histories (Linderman
290 et al. (2014); Huang et al. (2015); Arriola et al. (2014); Dávila et al. (2014); Petrie et al. (2016)).

291 **Discussion**

292 The distribution of influenza cases by birth year is consistent with subtype-level imprinting, whereby
293 initial infection with a subtype protects against future infections by the same subtype. The stronger
294 protective effect observed for primary H1N1 infection compared to primary H3N2 infection may be
295 caused by greater cross-protective responses to conserved epitopes. This is in line with previous work
296 modeling antibody titer dynamics that showed that protection conferred by H1N1 infection is longer-
297 lasting than protection conferred by H3N2 infection (Ranjeva et al. (2019)). Subtype-specific protection
298 is more specific than the previously reported group-level imprinting (Gostic et al. (2016)) but clearly

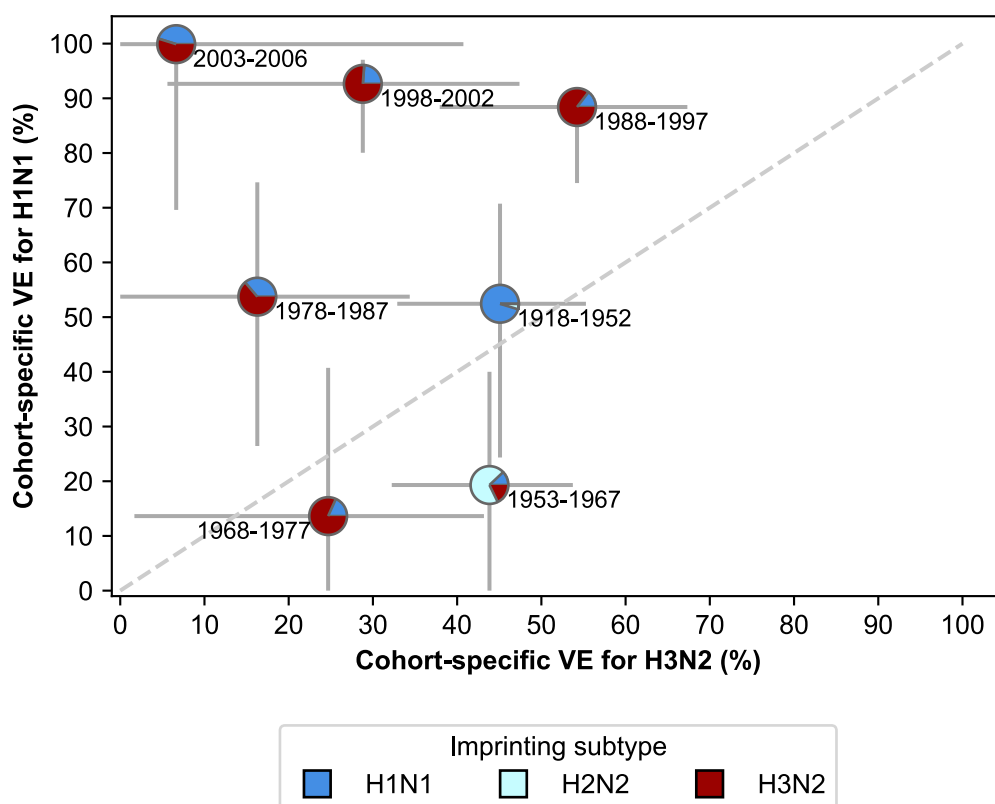


Figure 6. Birth-cohort-specific VE differs significantly between subtypes and birth cohorts. The location of each pie chart represents the H3N2 (x-axis) and H1N1 (y-axis) VE estimates for a birth cohort (indicated by text) obtained from our model excluding children <10 years old. Pie charts are colored by the probability of first infection by each subtype (i.e., imprinting probability). 95% confidence intervals of the VE estimates are indicated by light grey solid lines. The dashed grey line shows the diagonal where the VE estimate for H1N1 is equal to the VE estimate for H3N2.

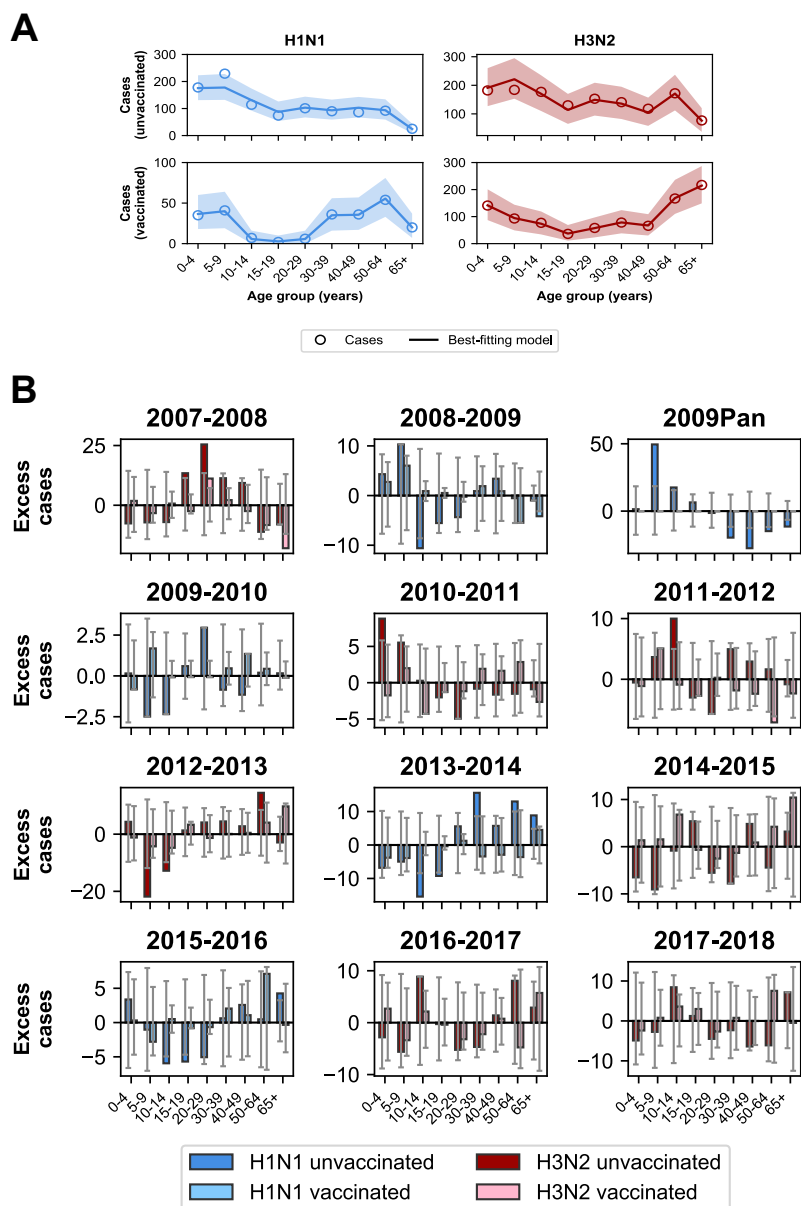


Figure 7. A. Best-fitting model accurately predicts the overall age distribution of cases across seasons and age groups. The best-fitting model includes the effects of demography, age, VE by age class, and subtype-specific HA imprinting. Each row depicts the age distribution of cases among unvaccinated (top) and vaccinated (bottom) individuals over all sampled seasons (2007-2008 through 2017-2018). Each column indicates H1N1 cases (left, blue) and H3N2 cases (right, red). Open circles represent observed cases, solid lines represent the predicted number of cases from the best-fitting model, the shaded area represents the 95% prediction interval of the best-fitting model. **B.** Excess cases of dominant subtype for each season. Each panel shows the excess cases of the dominant subtype for each season for each age group among unvaccinated (dark bars) and vaccinated (light bars) individuals. Excess cases are defined as the predicted number of cases from the best-fitting model - observed cases. Grey error bars show the 95% prediction interval.

299 arises from primary infection rather than any prior exposure.

300 In contrast to the clear role of the imprinting subtype in protection from infection, the model
301 implicates the imprinting strain or other attributes of exposure history in VE. Birth-cohort-specific VE
302 predicts the distribution of cases in older children and adults better than age-specific or imprinting-
303 subtype-specific VE. Although seasonal estimates of VE routinely stratify by age, shifts in VE from
304 one season to the next might be easier to interpret in light of infection history (e.g., Skowronski et al.
305 (2017b); Flannery et al. (2018)). The results suggest this effect may be complex, i.e., influenced by
306 strains' specific identities rather than merely their subtype. Our model cannot distinguish between
307 the possibility that the precise identity of the imprinting strain primarily determines later VE, or if
308 individuals' responses to vaccination are shaped by a particular succession of exposures, which will be
309 common to others in the same birth cohort. Regardless, variation in VE between birth cohorts appears
310 substantial and suggests a role for past exposure in the effectiveness of vaccination. This presents a
311 challenge for the improvement of vaccination strategies (Erbelding et al. (2018)).

312 Biases associated with our methodology and the vaccination history of our study population may
313 confound our estimates of VE. Potential selection and misclassification biases are associated with
314 studies that use influenza test-negative controls to control for differences in healthcare-seeking behavior
315 (Lewnard et al. (2018); Sullivan et al. (2016)). Because we also use test-negative controls to set our
316 null expectation for the distribution of cases among birth cohorts, our VE estimates are subject to these
317 biases as well. Moreover, our study population is heavily vaccinated, and the most participants are
318 frequent vaccinees (Figure 3-Supplement 3). Frequent vaccination has been associated with reduced
319 VE (McLean et al. (2014b); Saito et al. (2018); Skowronski et al. (2016)). Therefore, our estimates
320 may underestimate VE in less vaccinated populations. We observed an unusually high H1N1 VE in the
321 2003-2006 birth cohort. Because we restricted cases in this analysis to people ≥ 10 years old, this VE
322 estimate included data from only the 2013-2014 and 2015-2016 influenza seasons. No H1N1 cases
323 among vaccinated or unvaccinated individuals were observed in this birth cohort for those seasons,
324 which in turn led to this high estimate of H1N1 VE. To reduce stochastic effects, our estimates are
325 worth repeating in a larger population.

326 Incorporating differences in susceptibility based on exposure history might improve methods to
327 forecast influenza seasons. Our analysis of the relative risk of infection during the first half of each
328 season suggests more variation in the most susceptible age groups from season to season than previously
329 estimated (Worby et al. (2015)). While the smaller sample sizes in Marshfield compared to national
330 data create uncertainty in our estimates, the correlation between the relative risk and total fraction of
331 cases indicates that the age groups driving epidemics change from season to season. As our results
332 show, these differences in susceptibility may derive from differences in exposure history. Therefore,
333 incorporating information on exposure history into epidemic models may allow for more accurate
334 identification of at-risk populations.

335 While the rate of antigenic evolution affects the rate at which different populations become suscep-
336 tible to infection, the heterogeneity in susceptibility we observe here may also drive antigenic evolution.
337 This heterogeneity in susceptibility implies that influenza viruses face different selective pressures in
338 groups with different exposure histories (Cobey and Hensley (2017)). Recent research consistent with
339 this hypothesis has shown that sera isolated from different individuals can select for distinct influenza

340 escape mutants (Lee et al. (2019)). More careful study of how immune memory to influenza evolves
341 from infection and vaccination might improve understanding of influenza's evolution.

342 **Materials and Methods**

343 **Study cohort**

344 Cases of PCR-confirmed, medically attended influenza were identified from annual community cohorts
345 based on residency in the Marshfield Epidemiologic Study Area (MESA) in central Wisconsin. MESA
346 is a 14-ZIP-code geographic area surrounding Marshfield, Wisconsin, where nearly all residents receive
347 outpatient and inpatient care from the Marshfield Clinic Health System. For each influenza season
348 from 2007-2008 through 2017-2018, we identified a subset of MESA residents >6 months of age who
349 received routine care from the Marshfield Clinic. These individuals were eligible for recruitment into a
350 VE study if they sought care for acute respiratory illness during each influenza season. Most patients
351 with MAARI were recruited in the outpatient setting, but inpatient recruitment also occurred in 2007-08
352 and 2008-09. Recruitment occurred in primary care departments, including urgent care, pediatrics,
353 combined internal medicine and pediatrics, internal medicine, and family practice. The proportion
354 of patients with MAARI who were screened for enrollment varied by season. We excluded patients
355 recruited in an inpatient (hospital) setting.

356 Each season, recruitment began when influenza activity was detected in the community and usually
357 continued for 12-15 weeks. Symptom eligibility criteria varied by season but included fever/feverishness
358 or cough during most seasons. We retroactively standardized symptom eligibility criteria to only require
359 cough as a symptom. Individuals with illness duration >7 days were excluded. After obtaining informed
360 consent, a mid-turbinate swab was obtained for influenza detection. RT-PCR was performed using
361 CDC primers and probes to identify influenza cases, including type and subtype.

362 The Marshfield Clinic generally does not capture MAARI in nursing facilities with dedicated
363 medical staff, causing undersampling of the oldest age groups. We adjusted for this ("Age-specific
364 factors" below).

365 We considered subjects vaccinated if they received that season's influenza vaccine ≥ 14 days before
366 enrollment. For the 2009-2010 season, we only considered receipt of the 2009 monovalent vaccine.

367 **Calculating differences in the age distribution between seasons**

368 We defined the age distribution of each season as the number of cases of the dominant subtype in each
369 of nine age groups (0-4 year-olds, 5-9 year-olds, 10-14 year-olds, 15-19 year-olds, 20-29 year-olds,
370 30-39 year-olds, 40-49 year-olds, 50-64 year-olds, and >64 years old). The G-test of independence
371 was used to determine whether each pair of seasons had significantly different age distributions. We
372 considered differences significant if the Bonferroni-corrected p-value was <0.05.

373 **Calculating relative risk**

374 We used an approach similar to Worby et al. (2015) in calculating relative risk. We defined the midpoint
375 of each season as the week in which the cumulative number of cases of the dominant subtype exceeded
376 50% of the total for that season. Weeks before and after this point were assigned to the first and second
377 half of the season, respectively. We assigned each case to one of the five age groups used by Worby

378 et al. (2015) (0-4 year-olds, 5-17 year-olds, 18-49 year-olds, 50-64 year olds, and >64 years old). For
379 each age group g , we defined relative risk as

$$\frac{C_{\text{first},t,g}}{C_{\text{second},t,g}},$$

380 where $C_{\text{first},t,g}$ and $C_{\text{second},t,g}$ are the fraction of cases of the dominant subtype in age group g during
381 influenza season t that occurred during the first or second half of the season, respectively. A relative
382 risk >1 indicates that cases in an age group were more likely to occur during the first half of the season.

383 **Calculating imprinting probabilities**

384 **Seasonal intensity**

385 We define the intensity of an influenza season as the product of the mean fraction of patients with
386 influenza-like illness (ILI) and the percentage of specimens testing positive for influenza A that season,

$$I_t = \frac{\text{ILI}_t F_t}{N_t},$$

387 where ILI_t is the mean fraction of all patients with ILI in season t adjusted for differences in state
388 population size (CDC (2018)), F_t is the number of respiratory specimens testing positive for influenza
389 A in season t , and N_t is the total number of respiratory specimens tested in season t . For seasons
390 1997-1998 through 2017-2018, these data were obtained from the U.S. Outpatient Influenza-like Illness
391 Surveillance Network (ILINet) and the World Health Organization/National Respiratory and Enteric
392 Virus Surveillance System (WHO/NREVSS) Collaborating Labs (CDC (2018)). For seasons 1976-1977
393 through 1996-1997, we assumed that the mean ILI was equal to the mean of mean ILI for seasons
394 1997-1998 through 2017-2018. We obtained data on F_t and N_t for these seasons from Thompson et al.
395 (2003). We then normalized the intensity of each season by dividing I_t by the mean of I_t from the
396 1976-1977 through 2017-2018 seasons. For all seasons before 1976-1977, we assumed that the intensity
397 of influenza A equalled the mean intensity of seasons 1976-1977 through 2017-2018.

398 **Fraction of season experienced**

399 We define the fraction of a given influenza season $f_{w,t}$ occurring in week w of season t as

$$f_{w,t} = \frac{\text{ILI}_{w,t} F_{w,t}}{N_{w,t} \sum_{w'=w_0}^{w_f} \frac{\text{ILI}_{w',t} F_{w',t}}{N_{w',t}}},$$

where $\text{ILI}_{w,t}$ is the weighted fraction of all patients with ILI in week w of season t , $F_{w,t}$ is the number
of respiratory specimens testing positive for influenza A in week w of season t , and $N_{w,t}$ is the number
of specimens tested in week w of season t . $\sum_{w'=w_0}^{w_f} \frac{\text{ILI}_{w',t} F_{w',t}}{N_{w',t}}$ is the product of ILI and the fraction
of positive influenza A specimens summed over all weeks of the influenza season t , where w_0 is the
first week of the season and w_f is the final week of the season. We define the start of the influenza
season as week 40 of the calendar year, which usually falls at the beginning of October. For seasons
before 1997-1998, where weekly data is unavailable, we assume that the fraction of the influenza season
experienced in week w is

$$f_{w,t} = \bar{f}_{w,t},$$

400 where $\bar{f}_{w,t}$ is the mean fraction of the influenza season experienced at week w for all seasons after
401 1997-1998.

402 We use $f_{w,t}$ to calculate the fraction of an influenza season experienced by an individual born in
403 year y . We assume that people born in year y are born randomly throughout the year. We also assume
404 that due to maternal immunity, infants do not experience immunizing exposure to influenza until they
405 are at least 180 days old. Let $p_{y,w,t}$ be the proportion of individuals born in year y that are over 180 days
406 old in week w of season t and $e_{y,t}$ be the fraction of individuals born in year y exposed to influenza
407 season t . Then

$$e_{y,t} = \sum_{w=w_0}^{w_f} f_{w,t} p_{y,w,t}.$$

408 Imprinting probability

409 We emulate the approach of Gostic et al. (2016) in calculating the probability that people born in a
410 particular year had their initial influenza exposure to a particular subtype.

411 To obtain imprinting probabilities, we calculate the probability that an individual born in year y
412 receives their first influenza A exposure in influenza season t . Specifically, we consider two possible
413 scenarios. First, we assume that only infections result in an imprinting exposure. Second, we modify
414 our calculation to include the possibility that both vaccination and infection result in an imprinting
415 exposure.

416 We set the probability of infection for naive individuals at 0.28 (Bodewes et al. (2011); Gostic et al.
417 (2016)). Using this probability, we can calculate a per-season attack rate a assuming an exponential
418 hazard:

$$a = -\ln(0.72).$$

419 We then scale this attack rate by the intensity of influenza season t (I_t) and the fraction of influenza
420 season t experienced by an individual born in year y ($e_{y,t}$, "Seasonal intensity" above). The probability
421 that a naive individual born in year y is infected in influenza season t is

$$p_{y,t} = 1 - e^{-I_t e_{y,t} a}.$$

422 Considering only infection,

$$Pr(\text{unexposed}, t) \equiv N(t)$$

$$N(t = 0) = 1$$

$$Pr(\text{first exposure in season } t) = Pr(\text{infected}|\text{unexposed})Pr(\text{unexposed}) = p_{y,t} N(t)$$

$$N(t + 1) = N(t)(1 - p_{y,t})$$

423 We calculate subtype-specific imprinting probabilities by multiplying $p_{y,t} N(t)$ by the subtype frequencies
424 for each season (Figure 2-Supplement 1).

425 To incorporate vaccination, we make a simplifying assumption that for all seasons except the 2009
 426 pandemic and the 2009-2010 influenza seasons (discussed below), vaccination occurs before infection.
 427 We also consider that given vaccination coverage for a particular birth cohort and season ($c_{y,t}$), only a
 428 fraction of those individuals will be receiving their first vaccination because people who get vaccinated
 429 are more likely to get vaccinated again. We calculated this probability of first vaccination by age ($f_{a,t}$)
 430 using the vaccination status of children enrolled in our study (Figure 5-Supplement 7).

431 We track the fraction of a birth cohort naive to any exposure ($N(t)$ as above) and the fraction of
 432 a birth cohort naive to vaccination ($N_v(t)$). Therefore, to calculate imprinting probabilities, we first
 433 consider vaccination:

$$N(t = 0) = N_v(t = 0) = 1$$

$$Pr(\text{first vaccination in season } t) = \frac{Pr(\text{vaccinated})Pr(\text{first vaccination}|\text{vaccinated})}{Pr(\text{naive to vaccination})} = \frac{c_{y,t}f_{a,t}}{N_v(t)}$$

$$Pr(\text{first exposure via vaccination in season } t) = \frac{c_{y,t}f_{a,t}}{N_v(t)} N(t)$$

$$N_v(t + 1) = N_v(t) \left(1 - \frac{c_{y,t}f_{a,t}}{N_v(t)}\right)$$

434 Then, we update $N(t)$ to reflect vaccination and use this new value of $N(t)$ to calculate the fraction of
 435 people infected:

$$N(t) = N(t) \left(1 - \frac{c_{y,t}f_{a,t}}{N_v(t)}\right)$$

$$Pr(\text{first exposure via infection in season } t) = Pr(\text{infected}|\text{unexposed})Pr(\text{unexposed}) = p_{y,t}N(t)$$

$$N(t + 1) = N(t)(1 - p_{y,t})$$

436 During the 2009 H1N1 pandemic and 2009-2010 seasons, infection, vaccination with the seasonal
 437 vaccine, and vaccination with the monovalent vaccine occurred simultaneously. Therefore, we used
 438 weekly rates of vaccination and infection to estimate the probability that an individual's first exposure
 439 for that season was infection, seasonal vaccination, or monovalent vaccination.

440 Vaccination coverage

441 Seasonal influenza vaccination coverage for MESA Central was collected by age in the 2007-2008
 442 through 2017-2018 seasons using a real-time immunization registry (Irving et al. (2009)). Monovalent
 443 vaccination coverage for the 2009-2010 season was obtained by directly measuring monovalent vaccina-
 444 tion coverage in enrolled individuals and fitting a smoothing spline to the data (Figure 5-Supplement 6).

445 For seasons before 2007-2008, we used U.S. national data on vaccination coverage in children (2002-
 446 2003 through 2003-2004; Santibanez et al. (2006), 2004-2005 through 2006-2007; Santibanez et al.
 447 (2014)). We assumed that vaccination coverage in children (i.e., potentially imprinting vaccination) was
 448 0 before the 2002-2003 season, since that was the first season in which the Advisory Committee on
 449 Immunization Practices encouraged children 6-23 months old to receive influenza vaccination (Bridges
 450 et al. (2002)).

451 Model components

452 We aim to infer $p_{s,t,y,v}$, the predicted fraction of all PCR-confirmed influenza cases of dominant subtype
453 s in influenza season t among people born in year y with vaccine status v .

454 We normalize all models such that for each season t , $\sum_{y=1918}^{y_{\max}} p_{s,t,y,\text{unvac.}} + \sum_{y=1918}^{y_{\max}} p_{s,t,y,\text{vac.}} = 1$.
455 Let $p'_{s,t,y,v}$ be the unnormalized proportions. Then for season t ,

$$p_{s,t,y,v} = \frac{p'_{s,t,y,v}}{\sum_{y=1918}^{y_{\max}} p_{s,t,y,\text{unvac.}} + \sum_{y=1918}^{y_{\max}} p_{s,t,y,\text{vac.}}}.$$

For convenience, let $k_{M,t}$, the normalizing constant for season t in model M , be

$$k_{M,t} = \frac{1}{\sum_{y=1918}^{y_{\max}} p_{s,t,y,\text{unvac.}} + \sum_{y=1918}^{y_{\max}} p_{s,t,y,\text{vac.}}}.$$

456 Demography

457 We used Marshfield-specific data on the age distribution for each season (Kieke et al. (2015)). Individuals
458 ≥ 90 years old were grouped into a single age class. We therefore estimated the number of people in
459 each age by assuming a geometric decline in the age distribution. We converted the raw age distribution
460 for each season into a distribution by birth year by distributing people of a specific age into the two
461 possible birth years of that age in a specific season. Specifically, we assumed that people were born
462 uniformly throughout the year. We defined a breakpoint date prior to the start of the enrollment period
463 based on when the the 6 month-old age limit cutoff was set (e.g., if the breakpoint date was October 1,
464 then infants had to be 6 months old by that date to be eligible for enrollment). We used this date to
465 calculate the fraction of people of age a in season t who were born in year $t - y$ ($f_{1,a,t}$) or year $t - y - 1$
466 ($f_{2,a,t}$). A fraction $f_{1,a,t}$ of the total population of age a in season t was assigned to birth year $t - y$ and
467 $f_{2,a,t}$ to $t - y - 1$. Breakpoint dates ranged from September 1 through January 1 with the exception of
468 the pandemic season which had a breakpoint date of May 1, 2009. The start of the enrollment period
469 ranged from December to January with the exception of the 2009 pandemic season, when enrollment
470 began in May 2009. For the 2009 pandemic season, we assumed that the age distribution was the same
471 as the 2008-2009 season. The above procedure allows us to calculate $D_{t,y}$, the fraction of people born
472 in year y during influenza season t . Therefore,

$$p_{s,t,y,v} \propto D_{t,y}.$$

473 Age-specific factors

474 We modeled age-specific differences in influenza infection risk and healthcare-seeking behavior by
475 using parameters that represent the relative risk of medically attended influenza A infection in each
476 age group. These parameters combine the effects of underlying age-specific differences in influenza A
477 infection risk as well as age-specific differences in healthcare-seeking behavior. We consider the same
478 age groups as before (0-4 year-olds, 5-9 year-olds, 10-14 year-olds, 15-19 year-olds, 20-29 year-olds,
479 30-39 year-olds, 40-49 year-olds, 50-64 year-olds, and >64 years old). We choose 20-29 year-olds
480 as our reference age group. All age groups aside from 20-29 year-olds have an associated parameter
481 that models their risk of medically attended influenza A infection relative to 20-29 year-olds. These

482 parameters can take on any positive value. To map these age-specific parameters to birth cohorts, we
483 consider that each birth cohort has two possible ages in each season ($a1$ and $a2$). Let $G(a)$ be a function
484 that specifies the age group g of a given age a . Then $A_{t,y}$ the age-specific risk of medically attended
485 influenza A infection for a person born in year y in season t is

$$A_{t,y} = f_{a1,t,y}A_{G(a1)} + f_{a2,t,y}A_{G(a2)}$$

486 where $f_{a1,t,y}$ and $f_{a2,t,y}$ are the fractions of birth cohort y who are age $a1$ or $a2$ in influenza season t , and
487 $A_{G(a1)}$ and $A_{G(a2)}$ are the age-group-specific parameters for $a1$ and $a2$. With this, we model age-specific
488 effects as

$$p_{s,t,y,v} \propto A_{t,y}.$$

489 The relative rates at which different age groups were approached for study enrollment (the approach-
490 ment rate, p_{approach}) varied between seasons. Similarly, the relative rates at which different age groups
491 enrolled in the study after being approached (the enrollment rate, p_{enroll}) also varied between seasons.
492 Enrollment rates also varied between vaccinated and unvaccinated individuals.

493 We defined the approachment rate of an age group g in season t as

$$p_{\text{approach},t,g} = \frac{N_{\text{approached},t,g}}{N_{\text{MAARI},t,g}},$$

494 where $N_{\text{approached},t,g}$ is the number of people in age group g during season t who were approached for
495 enrollment, and $N_{\text{MAARI},t,g}$ is the total number of people in the Marshfield cohort who presented with
496 MAARI regardless of whether they were approached for enrollment.

497 We defined the enrollment rate of age group g in season t with vaccination status v as

$$p_{\text{enroll},t,g,v} = \frac{N_{\text{enrolled},t,g,v}}{N_{\text{approached},t,g,v}}$$

498 where $N_{\text{enrolled},t,g,v}$ is the number of people in age group g with vaccination status v who enrolled
499 in the study in season t , and $N_{\text{approached},t,g,v}$ is the number of people in age group g with vaccination
500 status v who were approached for enrollment in season t . Due to differences in data collection for the
501 2007-2008 and 2008-2009 seasons, complete vaccination records for eligible unenrolled individuals
502 were not available, so we assumed that the enrollment rates by age group and vaccination status in those
503 seasons were equal to the mean enrollment rate for each age group and vaccination status across all
504 other seasons.

505 We normalized $p_{\text{approach},t,g}$ by the value of $p_{\text{approach},t,g}$ for the reference age group (i.e., 20-29 year-
506 olds) in each season. Similarly, we normalized $p_{\text{enroll},t,g,v}$ to the value of $p_{\text{enroll},t,g,v}$ for unvaccinated
507 members of the reference age group for each season. This yielded the relative approachment and
508 enrollment rates $p'_{\text{approach},t,g}$ and $p'_{\text{enroll},t,g,v}$. We converted both $p'_{\text{approach},t,g}$ and $p'_{\text{enroll},t,g,v}$ to birth-year
509 specific covariates (i.e. covariates by y instead of g) using the same procedure described above for the
510 estimated age-specific parameters.

511 Finally, the study did not enroll residents of skilled nursing facilities with dedicated medical staff.
512 To account for this, we estimated the proportion of the population in nursing facilities within the study

513 area. We obtained the total number of beds in nursing facilities within the Marshfield study area in 2018
514 from the Wisconsin Department of Health Services (WDHS (2018)). We assumed that the total number
515 of beds did not change between 2007-2008 and 2017-2018. We also used data from the Centers for
516 Medicare and Medicaid Services (CMS (2015)) to calculate the percent of beds occupied in Wisconsin
517 nursing facilities by age for 2011 through 2014 and the fraction of people in a nursing facility by age
518 group. We used a smoothing spline to obtain the fraction of people of a given age in a nursing facility.
519 For seasons before 2010-2011 and after 2013-2014, we assumed that the fraction of people of a given
520 age in a nursing facility was the average value for 2011-2014. Given the total population of the study
521 area by age and season, we could then calculate the fraction of people in a given age a and season t
522 who are in nursing facilities ($s_{t,a}$). We convert this to a covariate by birth year ($s_{t,y}$) using the same
523 procedure described above for the age-specific parameters.

524 Thus, the combination of estimated age-specific effects and age-specific covariates is modeled as

$$p_{s,t,y,v} \propto A_{t,y} p'_{\text{approach},t,y} p'_{\text{enroll},t,y,v} (1 - s_{t,y}).$$

525 Vaccination

526 Vaccinated individuals may seek healthcare for symptomatic influenza at a different rate than unvac-
527 cinated individuals. Moreover, because vaccines are routinely recommended for individuals with
528 underlying health conditions, pre-existing susceptibility to acute respiratory infection among vaccinated
529 individuals may also differ from unvaccinated individuals. Let $R_{t,g}$ represent the fraction of vaccinated
530 individuals in age group g in season t that present with MAARI. We use test-negative controls to
531 estimate this as

$$R_{t,g} = \frac{v_{t,g}^-}{u_{t,g}^- + v_{t,g}^-},$$

532 where $v_{t,g}^-$ and $u_{t,g}^-$ are the number of vaccinated or unvaccinated individuals born in year g presenting
533 with MAARI and testing negative for influenza in season t . We compared this quantity to the vaccination
534 coverage of age group g in season t , $c_{t,g}$ (Figure 3-Supplement 2).

535 We converted $R_{t,g}$ to $R_{t,y}$ (i.e., to a birth cohort-indexed covariate) using the same procedure
536 described above to convert age group-specific parameters to birth-cohort-specific parameters.

537 We tested five different VE schemes: subtype-specific VE that remained constant across seasons
538 and cohorts (2 parameters), subtype-specific VE that varied between the age groups described above
539 (18 parameters), VE that varied between seasons (12 parameters), VE for each possible imprinting
540 subtype (6 parameters), and birth-cohort-specific VE (18 parameters). These VE parameters (V) reduce
541 the probability of medically attended influenza A infection among vaccinated individuals within a birth
542 cohort, i.e.,

$$p_{s,t,y,\text{vac}} \propto R_{t,y} V,$$
$$p_{s,t,y,\text{unvac}} \propto (1 - R_{t,y}),$$

543 where V depends on the specific implementation of VE used.

544 For constant VE, $V = V_s = 1 - v_s$.

545 For season-specific VE, $V = V_{s,t} = 1 - v_{s,t}$.

546 For age-specific VE, we use a similar approach as described above for the age-specific parameters.
547 We use the same age classes but do not consider a reference age class, so that each age group has an
548 associated VE parameter for each subtype. Therefore,

$$V = V_{s,t,y} = 1 - (f_{a1,t,y}v_{G(a1),s} + f_{a2,t,y}v_{G(a2),s}),$$

549 where $v_{G(a1),s}$ and $v_{G(a2),s}$ are age-specific VE parameters for $a1$ and $a2$. Recall that the function G
550 specifies an age group for a given age.

551 For imprinting-specific VE, we use the imprinting probabilities for each birth cohort described
552 above such that

$$V = V_{s,t,y} = \prod_{z \in \{H1N1, H2N2, H3N2\}} (1 - v_{s,z}m_{z,t,y}),$$

553 where $v_{s,z}$ is the VE among people imprinted to subtype z against infection by dominant subtype s , and
554 m_z is the imprinting probability for subtype z in season t for birth cohort y .

555 For birth-cohort-specific VE, we defined nine birth cohorts corresponding to the nine age groups we
556 used for the 2017-2018 season: 1918-1952, 1953-1967, 1968-1977, 1978-1987, 1988-1997, 1998-2002,
557 2003-2007, 2008-2012, and 2013-2017. Let $Q(y)$ be the birth cohort of people born in year y . Then

$$V = V_{s,y} = 1 - v_{Q(y),s},$$

558 where $v_{Q(y),s}$ is the VE among people in cohort $Q(y)$ against infection by dominant subtype s .

559 N2 imprinting

560 We consider that imprinting to N2 reduces a birth cohort's risk of H3N2 infection. Therefore,

$$p_{H3N2,t,y,v} \propto 1 - n_m(m_{H3N2,t,y} + m_{H2N2,t,y}),$$

561 where n_m is the strength of N2 imprinting, and $m_{H3N2,t,y}$ and $m_{H2N2,t,y}$ are the imprinting probabilities
562 of birth cohort y in season t to H3N2 and H2N2.

563 HA subtype imprinting

564 We consider that imprinting to HA reduces a birth cohort's risk of future infection from the same HA
565 subtype. Therefore,

$$p_{s,t,y,v} \propto 1 - h_s m_{s,t,y},$$

566 where h_s is the strength of HA imprinting for subtype s . and $m_{s,t,y}$ is the imprinting probability of birth
567 cohort y in season t to subtype s .

568 HA group imprinting

569 We consider that imprinting to HA reduces a birth cohort's risk of future infection from the viruses
570 within the same HA group. Therefore,

$$p_{H1N1,t,y,v} \propto 1 - g_1(m_{H1N1,t,y} + m_{H2N2,t,y}),$$

$$p_{H3N2,t,y,v} \propto 1 - g_2 m_{H3N2,t,y},$$

571 where g_1 is the strength of HA imprinting for group 1 viruses and g_2 is the strength of HA imprinting
572 for group 2 viruses.

573 Vaccine imprinting

574 We consider that imprinting via vaccination confers a fraction (x) of the protection conferred by infection.
575 If $x = 0$, vaccination prevents imprinting via infection without protecting against infection in future
576 seasons. If $x = 1$, vaccination imprints as well as infection. Because seasonal vaccines are polyvalent,
577 we assume that imprinting via vaccination protects against both H1N1 and H3N2 infections. Imprinting
578 via vaccination by the monovalent pandemic vaccine only protects against H1N1 infections. Therefore,
579 for subtype-specific imprinting,

$$p_{s,t,y,v} \propto 1 - x h_s m_{v,t,y},$$

580 where $m_{v,t,y}$ is the probability of imprinting via vaccination in season t for birth cohort y . Similarly, for
581 group-specific imprinting,

$$p_{H1N1,t,y,v} \propto 1 - x g_1 m_{v,t,y}$$

$$p_{H3N2,t,y,v} \propto 1 - x g_2 m_{v,t,y}.$$

582 In models including vaccine imprinting, the imprinting probabilities for infection differ from the
583 infection-only model. That is, we use the imprinting probabilities from Figure 5-Supplement 3 and not
584 the probabilities from Figure 2. We assume that the protection conferred by imprinting via vaccination
585 cannot exceed protection conferred by initial infection and therefore restrict x to lie between 0 and 1.

586 Model likelihood

587 Let $n_{s,t,y,v}$ be the number of PCR-confirmed influenza cases of dominant subtype s in influenza season t
588 among people born in year y with vaccination status v . The total number of PCR-confirmed cases of
589 dominant subtype s in season t is

$$N_{s,t} = \sum_{y=1918}^{y_{\max}} n_{s,t,y,\text{unvac.}} + \sum_{y=1918}^{y_{\max}} n_{s,t,y,\text{vac.}}$$

590 For models fitted to a restricted set of ages, we limited the cases for each season to the birth cohorts
591 that were guaranteed to meet the age requirements in that season.

592 We aim to infer $p_{s,t,y,v}$, the predicted fraction of all PCR-confirmed influenza cases of subtype s in
593 influenza season t among people born in year y with vaccination status v .

594 For a specific model M , we consider all possible model components j described above (demography,
595 age, vaccination, and imprinting). Then,

$$p_{s,t,y,v} = k_{M,t} \prod_j j M_j,$$

596 where M_j indicates whether model M contains component j (e.g., for HA subtype imprinting, $j =$
 597 $1 - h_s m_{s,t,y}$).

598 The likelihood for season t is given by the multinomial likelihood,

$$\mathcal{L}_t = \frac{N_{s,t}! p_{s,t,1918,\text{unvac.}}^{n_{s,t,1918,\text{unvac.}}} p_{s,t,1918,\text{vac.}}^{n_{s,t,1918,\text{vac.}}} \cdots p_{s,t,y_{\max,t},\text{unvac.}}^{n_{s,t,y_{\max,t},\text{unvac.}}} p_{s,t,y_{\max,t},\text{vac.}}^{n_{s,t,y_{\max,t},\text{vac.}}}}{n_{s,t,1918,\text{unvac.}}! n_{s,t,1918,\text{vac.}}! \cdots n_{s,t,y_{\max,t},\text{unvac.}}! n_{s,t,y_{\max,t},\text{vac.}}!},$$

599 where $y_{\max,t}$ is the maximum birth year possible for a specific season t .

600 The full model likelihood for all observed seasons is

$$\mathcal{L} = \prod_{t=2007-2008}^{2017-2018} \mathcal{L}_t.$$

601 We fitted the model to case data using the L-BFGS-B algorithm implemented in the R package
 602 *optimx*. We estimated 95% confidence intervals for parameters of the best-fitting model by evaluating
 603 likelihood profiles at 15 evenly spaced points and interpolating the entire profile using a smoothing
 604 spline.

605 Sensitivity analyses

606 Sensitivity to age groups

607 To test whether our models were sensitive to our choice of age groups, we fit revised versions of all our
 608 models with different age groups:

- 609 • 0-4 years, 5-17 years, 18-49 years, 50-64 years, and ≥ 65 years
- 610 • 0-4 years, 5-17 years, 18-64 years, and ≥ 65 years

611 These models with alternate age groupings were fitted to case data to determine whether our findings
 612 on the strength of protection from initial H1N1 and H3N2 infection significantly changed from our fits
 613 using the higher-resolution age grouping described above (Appendix 1 Table 3).

614 Sensitivity to sampling effort

615 Sampling effort was not even across seasons, and analysis of the number of influenza cases per sampling
 616 day suggested that a significant number of cases may have been missed at the beginning or end of a
 617 specific seasons (Figure 5-Supplement 1). As our analysis of relative risk indicates, different age groups
 618 are more susceptible during different points in the influenza season, and therefore missing data from
 619 the beginning or end of a season could introduce bias in the observed age distribution of cases.

620 To adjust for this, we simulated cases for seasons which did not have sufficient sampling of the start
 621 or end of the epidemic period. We considered a season sufficiently sampled if

- 622 • the number of cases per sampling day in the first week of the enrollment period was < 1 and
- 623 • the number of cases per sampling day in the last week of the enrollment period was < 1 .

624 To extrapolate the start of a season, we linearly regressed the number of cases of the dominant
625 subtype per sampling day for each week of the first half of the season and identified the week of the
626 season where the number of cases per sampling day fell below 1 (t_0). For each week from t_0 to the first
627 week of the enrollment period, we used the regression of cases per sampling day to calculate the number
628 of cases we expected to see in each week. Summing these yields the total number of unsampled cases
629 at the beginning of the season. We used a similar approach to extrapolate the number of unsampled
630 cases at the end of a season by instead regressing cases per sampling day for each week of the latter
631 half of the season. We did not extrapolate cases for the 2010-2011 season for this analysis since the
632 observed number of cases per sampling day did not follow a typical epidemic curve.

633 We stochastically assigned a birth year and vaccination status to these cases according to a multi-
634 nomial distribution. The success probabilities of this distribution were set using the age distribution
635 of cases of the dominant subtype from the first two weeks of the enrollment period (if extrapolating
636 the beginning of a season) or the last two weeks of the enrollment period (if extrapolating the end of a
637 season). Specifically, we calculated the distribution of observed cases in the first or last two weeks of
638 the enrollment period among nine age groups (described above in "Age-specific factors") with their
639 associated vaccination status. We then assumed that cases were uniformly distributed among all birth
640 years contained in an age group. This yielded a set of probabilities describing the probability of infection
641 given birth year and vaccination status in a specific season.

642 We sampled from these multinomial distributions 1000 times to obtain augmented datasets that
643 combined observed and extrapolated cases. For each replicate simulation, we calculated the age
644 distribution of cases for the entire season as well as the relative risk of each age group in the first versus
645 the latter half of the season (Figure 1-Supplement 2B). We also fitted the best-fitting model to 100 of
646 these datasets (excluding the 2010-2011 season) and recorded the estimated imprinting strength for
647 both H1N1 and H3N2 for each fit (Figure 5-Supplement 2).

648 **Calculating excess cases**

649 We defined excess cases for a given birth cohort or age group as the number of observed cases for that
650 birth cohort or age group minus the number of predicted cases for that age group. Predictions were
651 obtained by multiplying the multinomial probabilities produced by the model by the total number of
652 cases of the dominant subtype in each season. A 95% prediction interval was obtained by simulating 100
653 datasets using the multinomial probabilities from a specific model (Figure 6-Supplement 2, Figure 7).

654 To test whether recent infection might be confounding our estimates, we calculated the correlation
655 between excess cases in each birth cohort in each season with excess cases of the same birth cohort in
656 the next season with the same dominant subtype (Figure 5-Supplement 5).

657 **Code and data availability**

658 The code and data used to perform the analyses for this project are available at <https://github.com/cobeylab/FluAImprinting>.
659

660 **Ethics**

661 Human subjects: Study procedures for the vaccine effectiveness study was approved by the IRB at the
662 Marshfield Clinic Research Institute. Informed consent was obtained from all participants at the time of
663 enrollment into the vaccine effectiveness study. This analysis was subsequently approved by the IRB
664 with a waiver of informed consent. The analysis of data was approved by the University of Chicago
665 IRB.

666 **Acknowledgments**

667 We thank Jennifer King and Carla Rottscheit for their assistance in providing the data for this study
668 and Rohan Dandavati for compiling historical data on subtype frequencies and ILI. We thank Mar-
669 cos Vieira and Kangchon Kim for their assistance in calculating imprinting probabilities. This work
670 was completed with computational resources provided by the University of Chicago's Research Com-
671 puting Center. Funding for this project was provided by the National Institutes of Health (NIH),
672 Department of Health and Human Services, under grant DP2AI117921 (to SC) and CEIRS Contract
673 No. HHSN272201400005C (to SC). Centers for Disease Control (CDC) provided funding to Marsh-
674 field Clinic Research Institute for original enrollment and data collection to estimate effectiveness
675 (U01IP001038, U01IP000471, U01IP000471, U01CI000192). The funders had no role in study design,
676 data collection and analysis, decision to publish, or preparation of the manuscript.

677 **References**

- 678 **Ann J**, Papenburg J, Bouhy X, Rheume C, Hamelin ME, Boivin G. Molecular and antigenic evolution of
679 human influenza A/H3N2 viruses in Quebec, Canada, 2009-2011. *J Clin Virol.* 2012; 53(1):88–92. doi:
680 10.1016/j.jcv.2011.09.016.
- 681 **Arriola CS**, Brammer L, Epperson S, Blanton L, Kniss K, Mustaquim D, Steffens C, Dhara R, Leon M, Perez A,
682 Chaves SS, Katz J, Wallis T, Villanueva J, Xu X, Abd Elal AI, Gubareva L, Cox N, Finelli L, Bresee J, et al.
683 Update: influenza activity - United States, September 29, 2013-February 8, 2014. *MMWR Morbidity and mor-*
684 *tality weekly report.* 2014; 63(7):148–154. <https://www.ncbi.nlm.nih.gov/pubmed/24553198><https://www.ncbi.nlm.nih.gov/pmc/PMC4584759/>.
- 686 **Beauté J**, Zucs P, Korsun N, Bragstad K, Enouf V, Kossyvakis A, Griškevičius A, Olinger CM, Meijer A, Guiomar
687 R, Prosenc K, Staroňová E, Delgado C, Brytting M, Broberg E, European Influenza Surveillance N. Age-specific
688 differences in influenza virus type and subtype distribution in the 2012/2013 season in 12 European coun-
689 tries. *Epidemiology and infection.* 2015; 143(14):2950–2958. [https://www.ncbi.nlm.nih.gov/pubmed/](https://www.ncbi.nlm.nih.gov/pubmed/25648399)
690 [25648399](https://www.ncbi.nlm.nih.gov/pmc/PMC4595855/)<https://www.ncbi.nlm.nih.gov/pmc/PMC4595855/>, doi: 10.1017/S0950268814003422.
- 691 **Bedford T**, Riley S, Barr IG, Broor S, Chadha M, Cox NJ, Daniels RS, Gunasekaran CP, Hurt AC, Kelso A,
692 Klimov A, Lewis NS, Li X, McCauley JW, Odagiri T, Potdar V, Rambaut A, Shu Y, Skepner E, Smith DJ,
693 et al. Global circulation patterns of seasonal influenza viruses vary with antigenic drift. *Nature.* 2015; 523:217.
694 <https://doi.org/10.1038/nature14460>, doi: 10.1038/nature14460.
- 695 **Belongia EA**, Kieke BA, Donahue JG, Coleman LA, Irving SA, Meece JK, Vandermause M, Lindstrom S,
696 Gargiullo P, Shay DK. Influenza vaccine effectiveness in Wisconsin during the 2007-08 season: comparison
697 of interim and final results. *Vaccine.* 2011; 29(38):6558–63. doi: 10.1016/j.vaccine.2011.07.002.

- 698 **Belongia EA**, Kieke BA, Donahue JG, Greenlee RT, Balish A, Foust A, Lindstrom S, Shay DK. Effectiveness
699 of Inactivated Influenza Vaccines Varied Substantially with Antigenic Match from the 2004–2005 Season to
700 the 2006–2007 Season. *The Journal of Infectious Diseases*. 2009; 199(2):159–167. [https://doi.org/10.](https://doi.org/10.1086/595861)
701 [1086/595861](https://doi.org/10.1086/595861), doi: 10.1086/595861.
- 702 **Biggerstaff M**, Jhung MA, Reed C, Fry AM, Balluz L, Finelli L. Influenza-like illness, the time to seek healthcare,
703 and influenza antiviral receipt during the 2010–2011 influenza season—United States. *The Journal of infectious*
704 *diseases*. 2014; 210(4):535–544.
- 705 **Bodewes R**, de Mutsert G, van der Klis FRM, Ventresca M, Wilks S, Smith DJ, Koopmans M, Fouchier
706 RAM, Osterhaus ADME, Rimmelzwaan GF. Prevalence of Antibodies against Seasonal Influenza A and
707 B Viruses in Children in Netherlands. *Clinical and Vaccine Immunology*. 2011; 18(3):469–476. [https:](https://cvi.asm.org/content/cdli/18/3/469.full.pdf)
708 [//cvi.asm.org/content/cdli/18/3/469.full.pdf](https://cvi.asm.org/content/cdli/18/3/469.full.pdf), doi: 10.1128/cvi.00396-10.
- 709 **Bridges CB**, Fukuda K, Uyeki TM, Cox NJ, Singleton JA. Prevention and control of influenza. Recommendations
710 of the Advisory Committee on Immunization Practices (ACIP). *MMWR Recomm Rep*. 2002; 51(Rr-3):1–31.
- 711 **Brooks-Pollock E**, Tilston N, Edmunds WJ, Eames KTD. Using an online survey of healthcare-seeking behaviour
712 to estimate the magnitude and severity of the 2009 H1N1v influenza epidemic in England. *BMC Infectious*
713 *Diseases*. 2011; 11(1):68. <https://doi.org/10.1186/1471-2334-11-68>, doi: 10.1186/1471-2334-11-
714 68.
- 715 **Budd AP**, Beacham L, Smith CB, Garten RJ, Reed C, Kniss K, Mustaquim D, Ahmad FB, Cummings CN, Garg
716 S, Levine MZ, Fry AM, Brammer L. Birth Cohort Effects in Influenza Surveillance Data: Evidence that
717 First Influenza Infection Affects Later Influenza-Associated Illness. *The Journal of Infectious Diseases*. 2019;
718 <https://doi.org/10.1093/infdis/jiz201>, doi: 10.1093/infdis/jiz201.
- 719 **Caini S**, Spreuwenberg P, Kuszniarz GF, Rudi JM, Owen R, Pennington K, Wangchuk S, Gyeltshen S,
720 Ferreira de Almeida WA, Pessanha Henriques CM, Njouom R, Vernet MA, Fasce RA, Andrade W, Yu
721 H, Feng L, Yang J, Peng Z, Lara J, Bruno A, et al. Distribution of influenza virus types by age using
722 case-based global surveillance data from twenty-nine countries, 1999-2014. *BMC infectious diseases*.
723 2018; 18(1):269–269. <https://www.ncbi.nlm.nih.gov/pubmed/29884140>[https://www.ncbi.nlm.](https://www.ncbi.nlm.nih.gov/pmc/PMC5994061/)
724 [nih.gov/pmc/PMC5994061/](https://www.ncbi.nlm.nih.gov/pmc/PMC5994061/), doi: 10.1186/s12879-018-3181-y.
- 725 **CDC**, FluView National, Regional, and State Level Outpatient Illness and Viral Surveillance. Accessed 23-
726 October-2018; 2018. <https://gis.cdc.gov/grasp/fluview/fluportaldashboard.html>.
- 727 **CMS**, Nursing Home Compendium 2015 Edition. Accessed 30-September-2019; 2015. [https://www.](https://www.cms.gov/Medicare/Provider-Enrollment-and-Certification/CertificationandCompliance/downloads/nursinghomedatacompendium_508-2015.pdf)
728 [cms.gov/Medicare/Provider-Enrollment-and-Certification/CertificationandCompliance/](https://www.cms.gov/Medicare/Provider-Enrollment-and-Certification/CertificationandCompliance/downloads/nursinghomedatacompendium_508-2015.pdf)
729 [downloads/nursinghomedatacompendium_508-2015.pdf](https://www.cms.gov/Medicare/Provider-Enrollment-and-Certification/CertificationandCompliance/downloads/nursinghomedatacompendium_508-2015.pdf).
- 730 **Cobey S**, Koelle K. Capturing escape in infectious disease dynamics. *Trends Ecol Evol*. 2008; 23(10):572–7.
731 doi: 10.1016/j.tree.2008.06.008.
- 732 **Cobey S**, Hensley SE. Immune history and influenza virus susceptibility. *Current Opinion in Virology*.
733 2017; 22:105–111. <http://www.sciencedirect.com/science/article/pii/S1879625716302127>,
734 doi: <https://doi.org/10.1016/j.coviro.2016.12.004>.
- 735 **Davenport FM**, Hennessy AV. A serologic recapitulation of past experiences with influenza A; antibody response
736 to monovalent vaccine, vol. 104; 1956. doi: 10.1084/jem.104.1.85.

- 737 **Davenport FM**, Hennessy AV. Predetermination by infection and by vaccination of antibody response to influenza
738 virus vaccines. *J Exp Med*. 1957; 106(6):835–50. doi: 10.1084/jem.106.6.835.
- 739 **DiazGranados CA**, Dunning AJ, Kimmel M, Kirby D, Treanor J, Collins A, Pollak R, Christoff J, Earl J, Landolfi
740 V. Efficacy of high-dose versus standard-dose influenza vaccine in older adults. *New England Journal of*
741 *Medicine*. 2014; 371(7):635–645.
- 742 **Dávila J**, Chowell G, Borja-Aburto VH, Viboud C, Grajales Muñiz C, Miller M. Substantial Morbidity and Mortal-
743 ity Associated with Pandemic A/H1N1 Influenza in Mexico, Winter 2013-2014: Gradual Age Shift and Severity.
744 *PLoS currents*. 2014; 6:eurrents.outbreaks.a855a92f19db1d90ca955f5e908d6631. <https://www.ncbi.nlm.nih.gov/pubmed/24744975><https://www.ncbi.nlm.nih.gov/pmc/PMC3967911/>, doi: 10.1371/cur-
745 rents.outbreaks.a855a92f19db1d90ca955f5e908d6631.
746
- 747 **Englund JA**, Walter EB, Fairchok MP, Monto AS, Neuzil KM. A comparison of 2 influenza vaccine schedules
748 in 6- to 23-month-old children. *Pediatrics*. 2005; 115(4):1039–47. doi: 10.1542/peds.2004-2373.
- 749 **Erbelding EJ**, Post DJ, Stemmy EJ, Roberts PC, Augustine AD, Ferguson S, Paules CI, Graham BS, Fauci
750 AS. A Universal Influenza Vaccine: The Strategic Plan for the National Institute of Allergy and Infectious
751 Diseases. *The Journal of Infectious Diseases*. 2018 02; 218(3):347–354. [https://doi.org/10.1093/](https://doi.org/10.1093/infdis/jiy103)
752 [infdis/jiy103](https://doi.org/10.1093/infdis/jiy103), doi: 10.1093/infdis/jiy103.
- 753 **Flannery B**, Smith C, Garten RJ, Levine MZ, Chung JR, Jackson ML, Jackson LA, Monto AS, Martin ET,
754 Belongia EA, McLean HQ, Gaglani M, Murthy K, Zimmerman R, Nowalk MP, Griffin MR, Keipp Talbot
755 H, Treanor JJ, Wentworth DE, Fry AM. Influence of Birth Cohort on Effectiveness of 2015-2016 Influenza
756 Vaccine Against Medically Attended Illness Due to 2009 Pandemic Influenza A(H1N1) Virus in the United
757 States. *J Infect Dis*. 2018; 218(2):189–196. doi: 10.1093/infdis/jix634.
- 758 **Fonville JM**, Fraaij PLA, de Mutsert G, Wilks SH, van Beek R, Fouchier RAM, Rimmelzwaan GF. Anti-
759 genic Maps of Influenza A(H3N2) Produced With Human Antisera Obtained After Primary Infection. *The*
760 *Journal of Infectious Diseases*. 2015; 213(1):31–38. <https://doi.org/10.1093/infdis/jiv367>, doi:
761 10.1093/infdis/jiv367.
- 762 **Francis T**. On the doctrine of original antigenic sin. *Proceedings of the American Philosophical Society*. 1960;
763 104(6):572–578.
- 764 **Gaglani M**, Pruszynski J, Murthy K, Clipper L, Robertson A, Reis M, Chung JR, Piedra PA, Avadhanula
765 V, Nowalk MP, Zimmerman RK, Jackson ML, Jackson LA, Petrie JG, Ohmit SE, Monto AS, McLean HQ,
766 Belongia EA, Fry AM, Flannery B. Influenza Vaccine Effectiveness Against 2009 Pandemic Influenza A(H1N1)
767 Virus Differed by Vaccine Type During 2013-2014 in the United States. *J Infect Dis*. 2016; 213(10):1546–56.
768 doi: 10.1093/infdis/jiv577.
- 769 **Gagnon A**, Acosta E, Hallman S, Bourbeau R, Dillon LY, Ouellette N, Earn DJD, Herring DA, Inwood K,
770 Madrenas J, Miller MS. Pandemic Paradox: Early Life H2N2 Pandemic Influenza Infection Enhanced
771 Susceptibility to Death during the 2009 H1N1 Pandemic. *mBio*. 2018; 9(1):e02091–17. [https://mbio.asm.](https://mbio.asm.org/content/mbio/9/1/e02091-17.full.pdf)
772 [org/content/mbio/9/1/e02091-17.full.pdf](https://mbio.asm.org/content/mbio/9/1/e02091-17.full.pdf), doi: 10.1128/mBio.02091-17.
- 773 **Gagnon A**, Miller MS, Hallman SA, Bourbeau R, Herring DA, Earn DJD, Madrenas J. Age-Specific Mortality Dur-
774 ing the 1918 Influenza Pandemic: Unravelling the Mystery of High Young Adult Mortality. *PLOS ONE*. 2013;
775 8(8):e69586. <https://doi.org/10.1371/journal.pone.0069586>, doi: 10.1371/journal.pone.0069586.

- 776 **Goldstein E**, Cobey S, Takahashi S, Miller JC, Lipsitch M. Predicting the Epidemic Sizes of Influenza A/H1N1,
777 A/H3N2, and B: A Statistical Method. *PLOS Medicine*. 2011; 8(7):e1001051. [https://doi.org/10.1371/
778 journal.pmed.1001051](https://doi.org/10.1371/journal.pmed.1001051), doi: 10.1371/journal.pmed.1001051.
- 779 **Gostic KM**, Ambrose M, Worobey M, Lloyd-Smith JO. Potent protection against H5N1 and H7N9 influenza via
780 childhood hemagglutinin imprinting. *Science*. 2016; 354(6313):722–726. doi: 10.1126/science.aag1322.
- 781 **Griffin MR**, Monto AS, Belongia EA, Treanor JJ, Chen Q, Chen J, Talbot HK, Ohmit SE, Coleman LA, Lofthus
782 G, Petrie JG, Meece JK, Hall CB, Williams JV, Gargiullo P, Berman L, Shay DK. Effectiveness of non-
783 adjuvanted pandemic influenza A vaccines for preventing pandemic influenza acute respiratory illness visits in
784 4 U.S. communities. *PLoS One*. 2011; 6(8):e23085. doi: 10.1371/journal.pone.0023085.
- 785 **Groth SFdS**, Webster R. Disquisitions on original antigenic sin: I. Evidence in man. *Journal of Experimental
786 Medicine*. 1966; 124(3):331–345.
- 787 **Huang KYA**, Rijal P, Schimanski L, Powell TJ, Lin TY, McCauley JW, Daniels RS, Townsend AR. Focused
788 antibody response to influenza linked to antigenic drift. *The Journal of clinical investigation*. 2015; 125(7):2631–
789 2645.
- 790 **Huang QS**, Bandaranayake D, Wood T, Newbern EC, Seeds R, Ralston J, Waite B, Bissielo A, Prasad N, Todd
791 A, Jelley L, Gunn W, McNicholas A, Metz T, Lawrence S, Collis E, Retter A, Wong SS, Webby R, Bocacao J,
792 et al. Risk Factors and Attack Rates of Seasonal Influenza Infection: Results of the Southern Hemisphere
793 Influenza and Vaccine Effectiveness Research and Surveillance (SHIVERS) Seroepidemiologic Cohort Study.
794 *J Infect Dis*. 2019; 219(3):347–357. doi: 10.1093/infdis/jiy443.
- 795 **Irving SA**, Donahue JG, Shay DK, Ellis-Coyle TL, Belongia EA. Evaluation of self-reported and
796 registry-based influenza vaccination status in a Wisconsin cohort. *Vaccine*. 2009; 27(47):6546–9. doi:
797 10.1016/j.vaccine.2009.08.050.
- 798 **Jackson LA**, Jackson ML, Nelson JC, Neuzil KM, Weiss NS. Evidence of bias in estimates of influenza
799 vaccine effectiveness in seniors. *International Journal of Epidemiology*. 2005 12; 35(2):337–344. [https://doi.org/10.1093/ije/
800 //doi.org/10.1093/ije/dyi274](https://doi.org/10.1093/ije/dyi274), doi: 10.1093/ije/dyi274.
- 801 **Jackson LA**, Nelson JC, Benson P, Neuzil KM, Reid RJ, Psaty BM, Heckbert SR, Larson EB, Weiss NS.
802 Functional status is a confounder of the association of influenza vaccine and risk of all cause mortality in seniors.
803 *International Journal of Epidemiology*. 2005 12; 35(2):345–352. [https://doi.org/10.1093/ije/
804 doi: 10.1093/ije/dyi275](https://doi.org/10.1093/ije/dyi275).
- 805 **Jackson ML**, Chung JR, Jackson LA, Phillips CH, Benoit J, Monto AS, Martin ET, Belongia EA, McLean
806 HQ, Gaglani M, Murthy K, Zimmerman R, Nowalk MP, Fry AM, Flannery B. Influenza Vaccine Effec-
807 tiveness in the United States during the 2015-2016 Season. *N Engl J Med*. 2017; 377(6):534–543. doi:
808 10.1056/NEJMoa1700153.
- 809 **Khiabani H**, Farrell GM, St George K, Rabadan R. Differences in patient age distribution between in-
810 fluenza A subtypes. *PloS one*. 2009; 4(8):e6832–e6832. [https://www.ncbi.nlm.nih.gov/pubmed/
811 19718262](https://www.ncbi.nlm.nih.gov/pubmed/19718262)<https://www.ncbi.nlm.nih.gov/pmc/PMC2729409/>, doi: 10.1371/journal.pone.0006832.
- 812 **Kieke AL**, Kieke BA, Kopitzke SL, McClure DL, Belongia EA, VanWormer JJ, Greenlee RT. Validation of Health
813 Event Capture in the Marshfield Epidemiologic Study Area. *Clinical Medicine & Research*. 2015; 13(3-4):103–
814 111. <http://www.clinmedres.org/content/13/3-4/103.abstract>, doi: 10.3121/cmr.2014.1246.

- 815 **Laurie KL**, Guarnaccia TA, Carolan LA, Yan AWC, Aban M, Petrie S, Cao P, Heffernan JM, McVernon J,
816 Mosse J, Kelso A, McCaw JM, Barr IG. Interval Between Infections and Viral Hierarchy Are Determinants of
817 Viral Interference Following Influenza Virus Infection in a Ferret Model. *The Journal of infectious diseases*.
818 2015; 212(11):1701–1710. <https://www.ncbi.nlm.nih.gov/pubmed/25943206><https://www.ncbi.nlm.nih.gov/pmc/PMC4633756/>, doi: 10.1093/infdis/jiv260.
- 820 **Lee JKH**, Lam GKL, Shin T, Kim J, Krishnan A, Greenberg DP, Chit A. Efficacy and effectiveness of high-dose
821 versus standard-dose influenza vaccination for older adults: a systematic review and meta-analysis. *Expert*
822 *Review of Vaccines*. 2018; 17(5):435–443. <https://doi.org/10.1080/14760584.2018.1471989>, doi:
823 10.1080/14760584.2018.1471989.
- 824 **Lee JM**, Eguia R, Zost SJ, Choudhary S, Wilson PC, Bedford T, Stevens-Ayers T, Boeckh M, Hurt A, Lakdawala
825 SS, Hensley SE, Bloom JD. Mapping person-to-person variation in viral mutations that escape polyclonal
826 serum targeting influenza hemagglutinin. *bioRxiv*. 2019; [https://www.biorxiv.org/content/early/](https://www.biorxiv.org/content/early/2019/06/13/670497)
827 2019/06/13/670497, doi: 10.1101/670497.
- 828 **Lewnard JA**, Tedijanto C, Cowling BJ, Lipsitch M. Measurement of Vaccine Direct Effects Under the Test-
829 Negative Design. *American Journal of Epidemiology*. 2018 08; 187(12):2686–2697. [https://doi.org/10.](https://doi.org/10.1093/aje/kwy163)
830 1093/aje/kwy163, doi: 10.1093/aje/kwy163.
- 831 **Linderman SL**, Chambers BS, Zost SJ, Parkhouse K, Li Y, Herrmann C, Ellebedy AH, Carter DM, Andrews SF,
832 Zheng NY, Huang M, Huang Y, Strauss D, Shaz BH, Hodinka RL, Reyes-Terán G, Ross TM, Wilson PC, Ahmed
833 R, Bloom JD, et al. Potential antigenic explanation for atypical H1N1 infections among middle-aged adults dur-
834 ing the 2013–2014 influenza season. *Proceedings of the National Academy of Sciences*. 2014; 111(44):15798.
835 <http://www.pnas.org/content/111/44/15798.abstract>, doi: 10.1073/pnas.1409171111.
- 836 **Manicassamy B**, Medina RA, Hai R, Tsibane T, Stertz S, Nistal-Villán E, Palese P, Basler CF, García-Sastre
837 A. Protection of mice against lethal challenge with 2009 H1N1 influenza A virus by 1918-like and classical
838 swine H1N1 based vaccines. *PLoS pathogens*. 2010; 6(1):e1000745.
- 839 **McLean HQ**, Thompson MG, Sundaram ME, Kieke BA, Gaglani M, Murthy K, Piedra PA, Zimmerman RK,
840 Nowalk MP, Raviotta JM, Jackson ML, Jackson L, Ohmit SE, Petrie JG, Monto AS, Meece JK, Thaker
841 SN, Clippard JR, Spencer SM, Fry AM, et al. Influenza Vaccine Effectiveness in the United States During
842 2012–2013: Variable Protection by Age and Virus Type. *The Journal of Infectious Diseases*. 2014 11;
843 211(10):1529–1540. <https://doi.org/10.1093/infdis/jiu647>, doi: 10.1093/infdis/jiu647.
- 844 **McLean HQ**, Thompson MG, Sundaram ME, Meece JK, McClure DL, Friedrich TC, Belongia EA. Impact of
845 repeated vaccination on vaccine effectiveness against influenza A (H3N2) and B during 8 seasons. *Clinical*
846 *Infectious Diseases*. 2014; 59(10):1375–1385.
- 847 **Monto AS**, Koopman JS, Longini J I M. Tecumseh study of illness. XIII. Influenza infection and disease,
848 1976–1981. *Am J Epidemiol*. 1985; 121(6):811–22. doi: 10.1093/oxfordjournals.aje.a114052.
- 849 **Neuzil KM**, Jackson LA, Nelson J, Klimov A, Cox N, Bridges CB, Dunn J, DeStefano F, Shay D. Immunogenicity
850 and Reactogenicity of 1 versus 2 Doses of Trivalent Inactivated Influenza Vaccine in Vaccine-Naive 5–8-Year-
851 Old Children. *The Journal of Infectious Diseases*. 2006; 194(8):1032–1039. [https://doi.org/10.1086/](https://doi.org/10.1086/507309)
852 507309, doi: 10.1086/507309.
- 853 **O’Donnell CD**, Wright A, Vogel LN, Wei CJ, Nabel GJ, Subbarao K. Effect of Priming with H1N1 Influenza
854 Viruses of Variable Antigenic Distances on Challenge with 2009 Pandemic H1N1 Virus. *Journal of Vi-*

855 rology. 2012; 86(16):8625–8633. <https://jvi.asm.org/content/jvi/86/16/8625.full.pdf>, doi:
856 10.1128/jvi.00147-12.

857 **Ohmit SE**, Thompson MG, Petrie JG, Thaker SN, Jackson ML, Belongia EA, Zimmerman RK, Gaglani M,
858 Lamerato L, Spencer SM, Jackson L, Meece JK, Nowalk MP, Song J, Zervos M, Cheng PY, Rinaldo CR,
859 Clipper L, Shay DK, Piedra P, et al. Influenza vaccine effectiveness in the 2011–2012 season: protection against
860 each circulating virus and the effect of prior vaccination on estimates. *Clin Infect Dis*. 2014; 58(3):319–27.
861 doi: 10.1093/cid/cit736.

862 **Petrie JG**, Parkhouse K, Ohmit SE, Malosh RE, Monto AS, Hensley SE. Antibodies Against the Current
863 Influenza A(H1N1) Vaccine Strain Do Not Protect Some Individuals From Infection With Contemporary
864 Circulating Influenza A(H1N1) Virus Strains. *The Journal of infectious diseases*. 2016; 214(12):1947–
865 1951. <https://www.ncbi.nlm.nih.gov/pubmed/27923954>[https://www.ncbi.nlm.nih.gov/pmc/](https://www.ncbi.nlm.nih.gov/pmc/PMC5142093/)
866 [PMC5142093/](https://www.ncbi.nlm.nih.gov/pmc/PMC5142093/), doi: 10.1093/infdis/jiw479.

867 **Ranjeva S**, Subramanian R, Fang VJ, Leung GM, Ip DKM, Perera RAPM, Peiris JSM, Cowling BJ, Cobey S.
868 Age-specific differences in the dynamics of protective immunity to influenza. *Nature Communications*. 2019;
869 10(1):1660. <https://doi.org/10.1038/s41467-019-09652-6>, doi: 10.1038/s41467-019-09652-6.

870 **Reed C**, Chaves SS, Daily Kirley P, Emerson R, Aragon D, Hancock EB, Butler L, Baumbach J, Hollick G, Bennett
871 NM, Laidler MR, Thomas A, Meltzer MI, Finelli L. Estimating influenza disease burden from population-based
872 surveillance data in the United States. *PLoS One*. 2015; 10(3):e0118369. doi: 10.1371/journal.pone.0118369.

873 **Saito N**, Komori K, Suzuki M, Kishikawa T, Yasaka T, Ariyoshi K. Dose-Dependent Negative Effects of Prior
874 Multiple Vaccinations Against Influenza A and Influenza B Among Schoolchildren: A Study of Kamigoto
875 Island in Japan During the 2011–2012, 2012–2013, and 2013–2014 Influenza Seasons. *Clinical Infectious*
876 *Diseases*. 2018; 67(6):897–904.

877 **Santibanez TA**, Lu PJ, O’Halloran A, Meghani A, Grabowsky M, Singleton JA. Trends in Childhood In-
878 fluenza Vaccination Coverage—U.S., 2004–2012. *Public Health Reports*. 2014; 129(5):417–427. doi:
879 10.1177/003335491412900505, pMID: 25177053.

880 **Santibanez TA**, Santoli JM, Bridges CB, Euler GL. Influenza Vaccination Coverage of Children Aged 6
881 to 23 Months: The 2002–2003 and 2003–2004 Influenza Seasons. *Pediatrics*. 2006; 118(3):1167–1175.
882 <https://pediatrics.aappublications.org/content/118/3/1167>, doi: 10.1542/peds.2006-0831.

883 **Skowronski DM**, Chambers C, De Serres G, Sabaiduc S, Winter AL, Dickinson JA, Gubbay JB, Fonseca K,
884 Drews SJ, Charest H, Martineau C, Krajdén M, Petric M, Bastien N, Li Y, Smith DJ. Serial Vaccination and
885 the Antigenic Distance Hypothesis: Effects on Influenza Vaccine Effectiveness During A(H3N2) Epidemics in
886 Canada, 2010–2011 to 2014–2015. *J Infect Dis*. 2017; 215(7):1059–1099. doi: 10.1093/infdis/jix074.

887 **Skowronski DM**, Chambers C, Sabaiduc S, De Serres G, Winter AL, Dickinson JA, Gubbay JB, Drews SJ,
888 Martineau C, Charest H, Krajdén M, Bastien N, Li Y. Beyond Antigenic Match: Possible Agent-Host and
889 Immuno-epidemiological Influences on Influenza Vaccine Effectiveness During the 2015–2016 Season in
890 Canada. *J Infect Dis*. 2017; 216(12):1487–1500. doi: 10.1093/infdis/jix526.

891 **Skowronski DM**, Chambers C, Sabaiduc S, De Serres G, Winter AL, Dickinson JA, Krajdén M, Gubbay JB,
892 Drews SJ, Martineau C, et al. A perfect storm: impact of genomic variation and serial vaccination on low
893 influenza vaccine effectiveness during the 2014–2015 season. *Clinical Infectious Diseases*. 2016; 63(1):21–32.

- 894 **Smith DJ**, Lapedes AS, de Jong JC, Bestebroer TM, Rimmelzwaan GF, Osterhaus AD, Fouchier RA. Mapping
895 the antigenic and genetic evolution of influenza virus. *Science*. 2004; 305(5682):371–6. doi: 10.1126/sci-
896 ence.1097211.
- 897 **Smith DJ**, Forrest S, Ackley DH, Perelson AS. Variable efficacy of repeated annual influenza vaccination.
898 *Proceedings of the National Academy of Sciences*. 1999; 96(24):14001–14006. [https://www.pnas.org/
899 content/96/24/14001](https://www.pnas.org/content/96/24/14001), doi: 10.1073/pnas.96.24.14001.
- 900 **Sullivan SG**, Tchetgen Tchetgen EJ, Cowling BJ. Theoretical Basis of the Test-Negative Study Design for
901 Assessment of Influenza Vaccine Effectiveness. *American journal of epidemiology*. 2016; 184(5):345–
902 353. <https://www.ncbi.nlm.nih.gov/pubmed/27587721>[https://www.ncbi.nlm.nih.gov/pmc/
903 PMC5013887/](https://www.ncbi.nlm.nih.gov/pmc/PMC5013887/), doi: 10.1093/aje/kww064.
- 904 **Thompson WW**, Shay DK, Weintraub E, Brammer L, Cox N, Anderson LJ, Fukuda K. Mortality Associated
905 With Influenza and Respiratory Syncytial Virus in the United States. *JAMA*. 2003; 289(2):179–186. <https://doi.org/10.1001/jama.289.2.179>, doi: 10.1001/jama.289.2.179.
- 907 **Treanor JJ**, Talbot HK, Ohmit SE, Coleman LA, Thompson MG, Cheng PY, Petrie JG, Lofthus G, Meece
908 JK, Williams JV, Berman L, Breese Hall C, Monto AS, Griffin MR, Belongia E, Shay DK. Effectiveness of
909 seasonal influenza vaccines in the United States during a season with circulation of all three vaccine strains.
910 *Clin Infect Dis*. 2012; 55(7):951–9. doi: 10.1093/cid/cis574.
- 911 **Van Caunteren D**, Vaux S, de Valk H, Le Strat Y, Vaillant V, Lévy-Bruhl D. Burden of influenza, healthcare
912 seeking behaviour and hygiene measures during the A(H1N1)2009 pandemic in France: a population based
913 study. *BMC Public Health*. 2012; 12(1):947. <https://doi.org/10.1186/1471-2458-12-947>, doi:
914 10.1186/1471-2458-12-947.
- 915 **WDHS**, Nursing Home Directory. Accessed 30-September-2019; 2018. [https://www.dhs.wisconsin.gov/
916 guide/nursing-home.htm](https://www.dhs.wisconsin.gov/guide/nursing-home.htm).
- 917 **Worby CJ**, Chaves SS, Wallinga J, Lipsitch M, Finelli L, Goldstein E. On the relative role of different age
918 groups in influenza epidemics. *Epidemics*. 2015; 13:10–16. [https://www.ncbi.nlm.nih.gov/pubmed/
919 26097505](https://www.ncbi.nlm.nih.gov/pubmed/26097505)<https://www.ncbi.nlm.nih.gov/pmc/PMC4469206/>, doi: 10.1016/j.epidem.2015.04.003.
- 920 **Worobey M**, Han GZ, Rambaut A. Genesis and pathogenesis of the 1918 pandemic H1N1 influenza A virus.
921 *Proceedings of the National Academy of Sciences of the United States of America*. 2014; 111(22):8107–
922 8112. <https://www.ncbi.nlm.nih.gov/pubmed/24778238>[https://www.ncbi.nlm.nih.gov/pmc/
923 PMC4050607/](https://www.ncbi.nlm.nih.gov/pmc/PMC4050607/), doi: 10.1073/pnas.1324197111.
- 924 **Wu JT**, Ma ES, Lee CK, Chu DK, Ho PL, Shen AL, Ho A, Hung IF, Riley S, Ho LM, Lin CK, Tsang T, Lo SV,
925 Lau YL, Leung GM, Cowling BJ, Malik Peiris JS. The infection attack rate and severity of 2009 pandemic
926 H1N1 influenza in Hong Kong. *Clin Infect Dis*. 2010; 51(10):1184–91. doi: 10.1086/656740.
- 927 **Wu S**, L VANA, Wang L, McDonald SA, Pan Y, Duan W, Zhang L, Sun Y, Zhang Y, Zhang X, Pilot E, Krafft
928 T, W VDH, MAB VDS, Yang P, Wang Q. Estimated incidence and number of outpatient visits for seasonal
929 influenza in 2015–2016 in Beijing, China. *Epidemiology and infection*. 2017; 145(16):3334–3344. doi:
930 10.1017/s0950268817002369.
- 931 **Zimmerman RK**, Nowalk MP, Chung J, Jackson ML, Jackson LA, Petrie JG, Monto AS, McLean HQ, Belon-
932 gia EA, Gaglani M, Murthy K, Fry AM, Flannery B, Investigators ftUFV. 2014–2015 Influenza Vaccine

933 Effectiveness in the United States by Vaccine Type. *Clinical Infectious Diseases*. 2016; 63(12):1564–1573.
934 <https://doi.org/10.1093/cid/ciw635>, doi: 10.1093/cid/ciw635.

935 **Supplementary tables and figures**

Appendix 1 Table 1. Estimates of parameters shared by the age-specific VE and birth-cohort-specific VE models.

	Model with age-specific VE, age ≥ 6 months (MLE 95% CI)	Model with age-specific VE, age ≥ 10 years (MLE, 95% CI)	Model with age-specific VE, age <65 years (MLE, 95% CI)	Model with age-specific VE, age 10-64 years (MLE, 95% CI)	Model with birth-cohort-specific VE, age ≥ 10 years (MLE 95% CI)
Imprinting protection (%)					
H1	66 (53, 77)	53 (32, 69)	64 (47, 77)	50 (23, 70)	54 (32, 70)
H3	33 (17, 46)	42 (24, 56)	34 (18, 47)	41 (22, 55)	41 (22, 56)
N2	0 (0, 7)	0 (0, 11)	0 (0, 8)	0 (0, 10)	0 (0, 11)
Age-specific risk of medically attended influenza A infection					
0-4 years	3.0 (2.5, 3.6)	N.A.	3.0 (2.5, 3.6)	N.A.	N.A.
5-9 years	2.6 (2.2, 3.0)	N.A.	2.5 (2.2, 3.0)	N.A.	N.A.
10-14 years	1.7 (1.4, 2.0)	1.8 (1.5, 2.1)	1.7 (1.4, 2.0)	1.8 (1.5, 2.1)	1.8 (1.5, 2.1)
15-19 years	1.2 (1.0, 1.5)	1.3 (1.0, 1.5)	1.2 (1.0, 1.5)	1.3 (1.0, 1.5)	1.3 (1.1, 1.6)
30-39 years	1.1 (0.9, 1.3)	1.1 (0.9, 1.3)	1.1 (0.9, 1.3)	1.1 (0.9, 1.3)	1.1 (0.9, 1.3)
40-49 years	0.9 (0.7, 1.1)	0.9 (0.8, 1.1)	0.9 (0.7, 1.1)	0.9 (0.8, 1.1)	0.9 (0.8, 1.1)
50-64 years	1.0 (0.8, 1.3)	0.9 (0.8, 1.2)	1.0 (0.8, 1.3)	1.0 (0.8, 1.2)	0.9 (0.8, 1.1)
65+ years	1.6 (1.2, 2.1)	1.4 (1.0, 1.8)	N.A.	N.A.	1.5 (1.1, 1.9)

Appendix 1 Table 2. Estimates of age-specific VE parameters in models fitted to different age groups.

	Model with age-specific VE, age ≥ 6 months (MLE 95% CI)	Model with age-specific VE, age ≥ 10 years (MLE, 95% CI)	Model with age-specific VE, age <65 years (MLE, 95% CI)	Model with age-specific VE, age 10-64 years (MLE, 95% CI)
Age-specific VE against H1N1 (%)				
0-4 years	69 (56, 84)	N.A.	68 (55, 83)	N.A.
5-9 years	26 (0, 48)	N.A.	24 (0, 47)	N.A.
10-14 years	92 (80, 96)	94 (82, 98)	92 (80, 96)	93 (81, 97)
15-19 years	86 (62, 95)	87 (64, 95)	86 (61, 95)	86 (62, 95)
20-29 years	84 (65, 91)	84 (65, 91)	83 (63, 90)	83 (64, 90)
30-39 years	8 (0, 37)	12 (0, 40)	5 (0, 35)	8 (0, 38)
40-49 years	18 (0, 45)	19 (0, 46)	14 (0, 42)	15 (0, 43)
50-64 years	32 (7, 51)	30 (4, 50)	28 (2, 48)	27 (0, 48)
65+ years	50 (16, 71)	56 (25, 75)	N.A.	N.A.
Age-specific VE against H3N2 (%)				
0-4 years	58 (48, 67)	N.A.	58 (48, 67)	N.A.
5-9 years	45 (31, 58)	N.A.	45 (30, 57)	N.A.
10-14 years	23 (0, 41)	26 (3, 45)	22 (0, 41)	25 (2, 44)
15-19 years	31 (3, 53)	35 (8, 56)	30 (2, 53)	34 (6, 55)
20-29 years	34 (11, 51)	37 (16, 53)	33 (11, 51)	36 (15, 53)
30-39 years	10 (0, 31)	15 (0, 35)	9 (0, 30)	14 (0, 34)
40-49 years	36 (15, 52)	42 (23, 57)	36 (15, 52)	42 (23, 57)
50-64 years	47 (35, 56)	50 (38, 59)	47 (35, 57)	49 (38, 59)
65+ years	41 (24, 54)	39 (22, 53)	N.A.	N.A.

Appendix 1 Table 3. Estimates of imprinting protection for models with different age groups.

Age groups (years)	Best-fitting model	H1 imprinting protection (% , 95% CI)	H3 imprinting protection (% , 95% CI)
0-4, 5-17, 18-64, 65+	Demography, age, HA imprinting, age-specific VE	56 (40, 68)	36 (25, 46)
0-8, 9-17, 18-49, 50-64, 65+	Demography, age, HA imprinting, age-specific VE	62 (47, 74)	35 (21, 48)

Appendix 1 Table 4. Estimates for VE from model with birth-cohort-specific VE fitted to people ≥ 10 years old.

Birth cohort	H1N1 VE (% , MLE, 95% CI)	H3N2 VE (% , MLE, 95% CI)
2003-2006	100 (70, 100)	7 (0, 41)
1998-2002	93 (80, 97)	29 (6, 47)
1988-1997	88 (75, 92)	54 (38, 67)
1978-1987	54 (26, 75)	16 (0, 34)
1968-1977	14 (0, 41)	25 (2, 43)
1953-1967	19 (0, 40)	44 (32, 54)
1918-1952	52 (24, 71)	45 (33, 55)

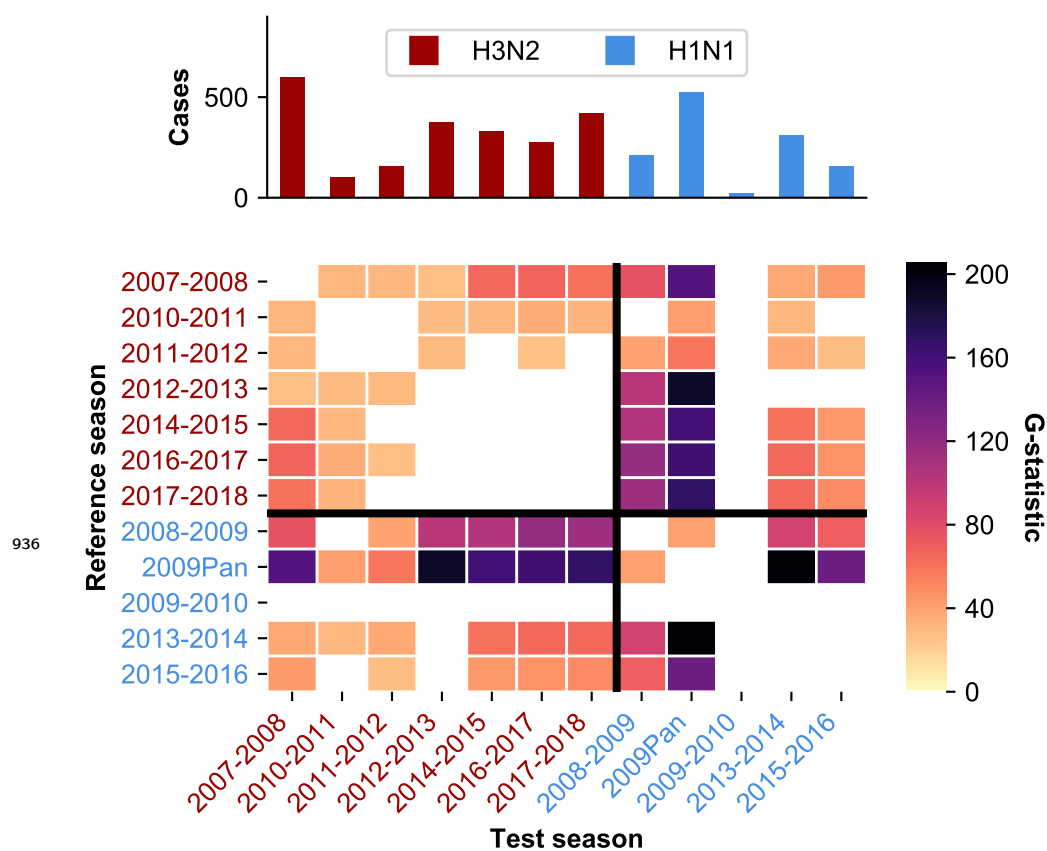


Figure 1-Supplement 1. Seasons differ significantly in their age distributions. Colored cells indicate that two seasons have significantly different age distributions (Bonferroni-corrected $p < 0.05$), and color intensity shows the observed G-test statistic (Materials and Methods: "Calculating differences in the age distribution between seasons."). White cells denote seasons that did not have significantly different age distributions from each other. The dominant subtype of each season is indicated by the label color.

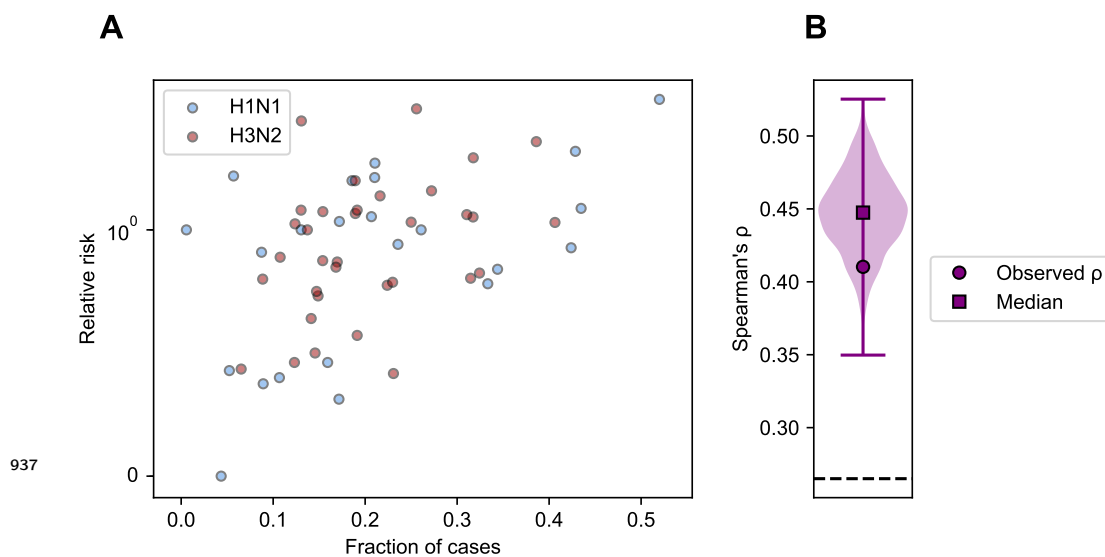


Figure 1–Supplement 2. A. Each point shows an age group’s relative risk of infection during the first half compared to the second half of an epidemic period (y-axis) and the fraction of cases belonging to that age group (x-axis) (Materials and Methods: "Calculating relative risk"). Points are colored by the dominant subtype of the season. **B.** To account for potential undersampling of cases at the beginning and end of specific seasons, we simulated 1000 replicate epidemics (Materials and Methods: "Sensitivity to sampling effort") and calculated the same correlation as in panel A. The range is indicated by a vertical line and the median by a square. Horizontal dashed black line indicates the critical value of ρ below which the correlation is not significant.

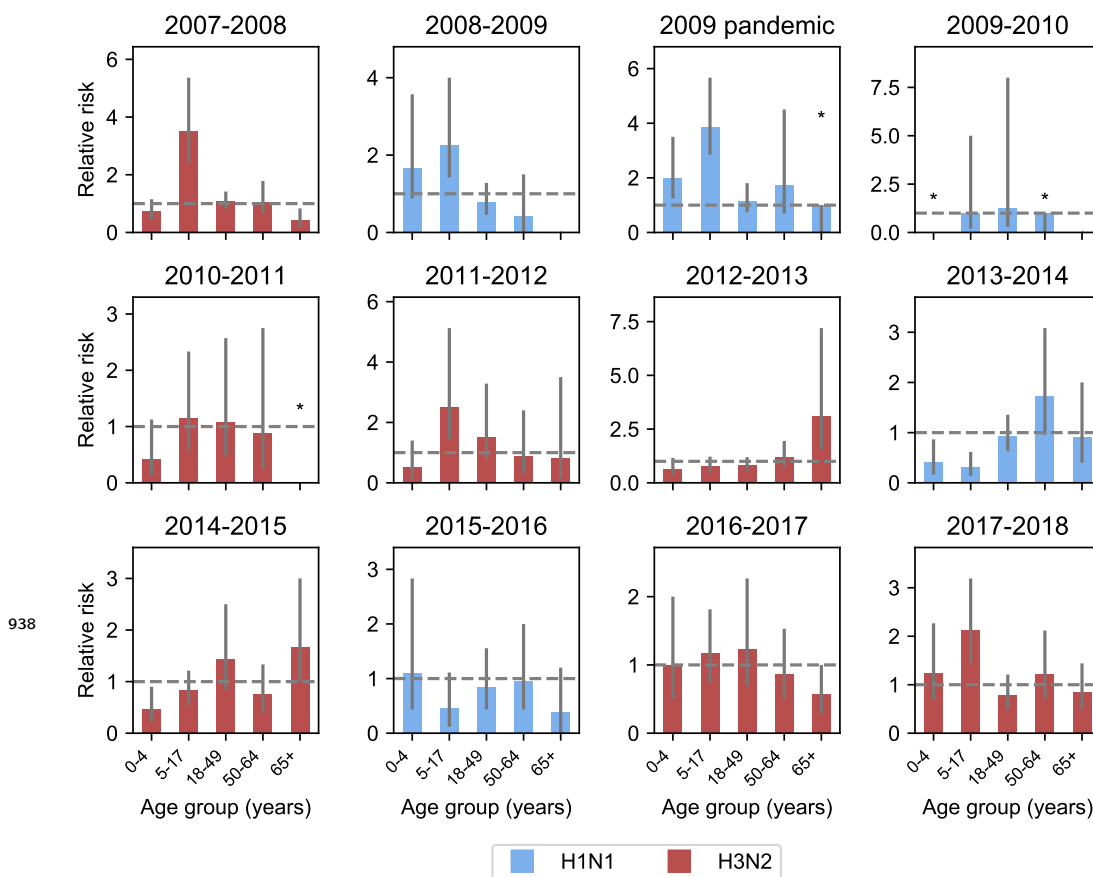


Figure 1-Supplement 3. Each panel shows the relative risk of infection in the first versus the second half of an epidemic for different age groups in each season (Materials and Methods: "Calculating relative risk"). Relative risk greater than 1 (indicated by the grey dashed line) means that an age group was more likely to be infected at during the first rather than second half of an epidemic. Age groups with no cases in the latter half of a season are indicated by asterisks and no bar. The dominant subtype of each subtype is indicated by the bar color. 95% binomial confidence intervals are indicated by grey vertical lines. Bars with asterisks over them indicate that the 95% confidence interval includes the scenario where all cases occur in the first half of the season.

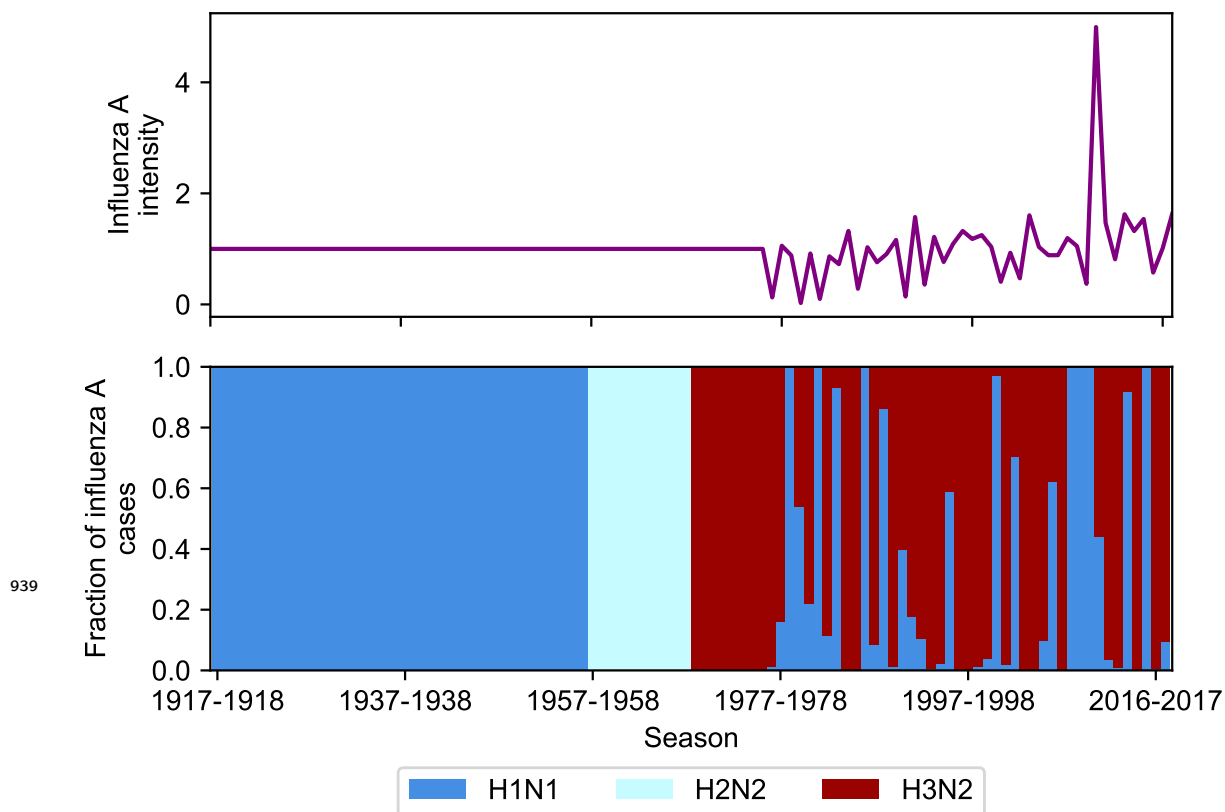


Figure 2–Supplement 1. The intensity (top panel) and subtype frequencies (bottom panel) of influenza A seasons in the United States. Intensity is measured as the product of influenza-like illness (ILI) and the fraction of respiratory specimens testing positive for influenza A in national surveillance data (Materials and Methods: "Seasonal intensity"). This is normalized to the average intensity value between 1977 and 2017-2018. Seasons before 1977 where United States ILI surveillance data are unavailable are assumed to have an intensity score of 1 (i.e., the average score over all other seasons). Subtype frequencies were obtained from national surveillance data before the 2007-2008 season and directly from the Marshfield studies afterwards.

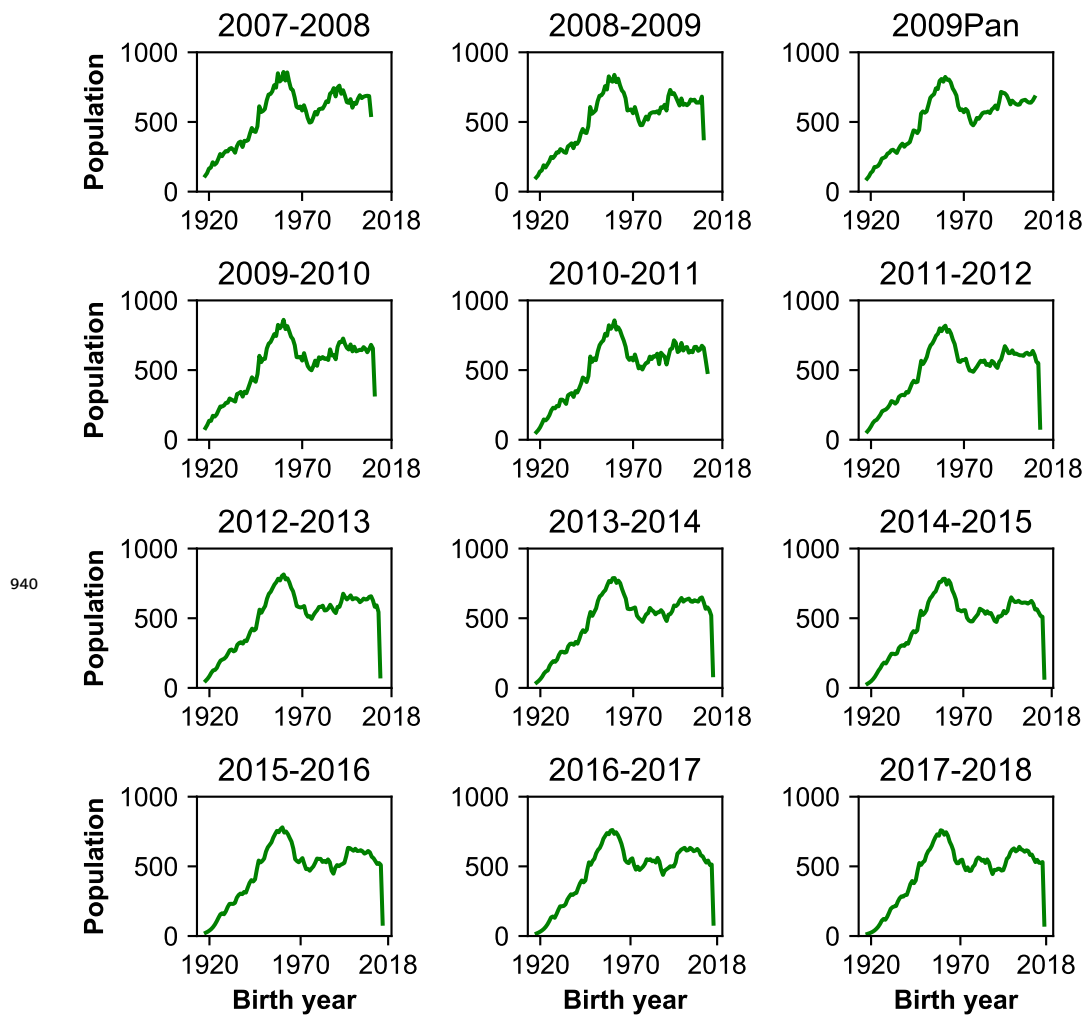


Figure 3–Supplement 1. Each panel shows the population distribution of all individuals in the study area who met the age criteria for study enrollment. People under 6 months old at the start of the sampling period in a season were not eligible to participate.

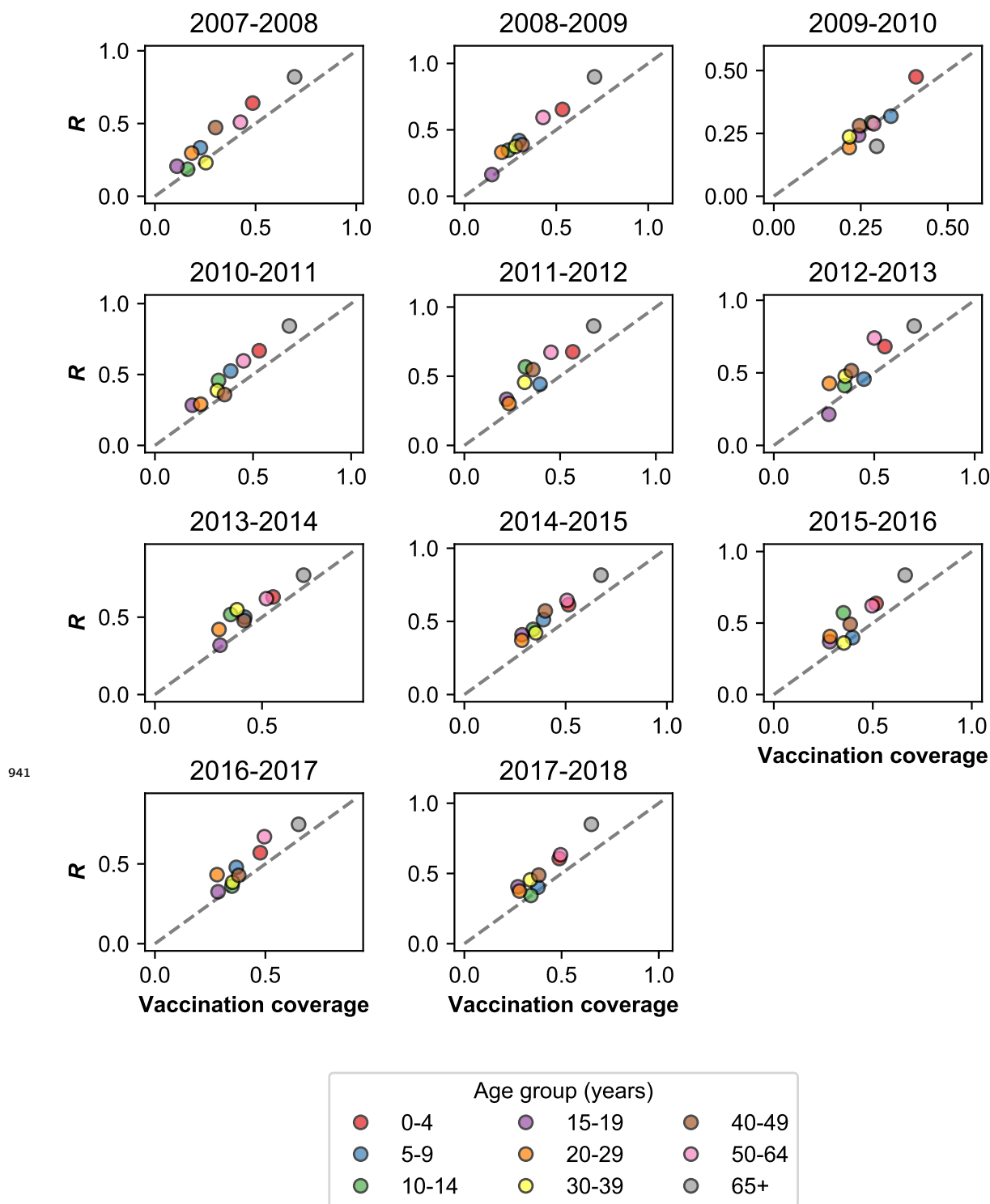


Figure 3-Supplement 2. Vaccinated individuals seek healthcare for MAARI at a higher rate than predicted by vaccination coverage. We measured the fraction of vaccinated people among all who presented with MAARI and tested negative for influenza ($R = \frac{\text{Vaccinated test-negative controls}}{\text{Unvaccinated test-negative controls} + \text{Vaccinated test-negative controls}}$, Materials and Methods: "Vaccination"). This is plotted against vaccination coverage by season for different age groups. The dashed grey line shows where R and vaccination coverage are equal. Vaccination coverage for the 2009-2010 season uses monovalent vaccination coverage estimated directly from all individuals with MAARI. We do not show the 2009 pandemic season because the monovalent vaccine was not distributed until the second wave of the pandemic.

942

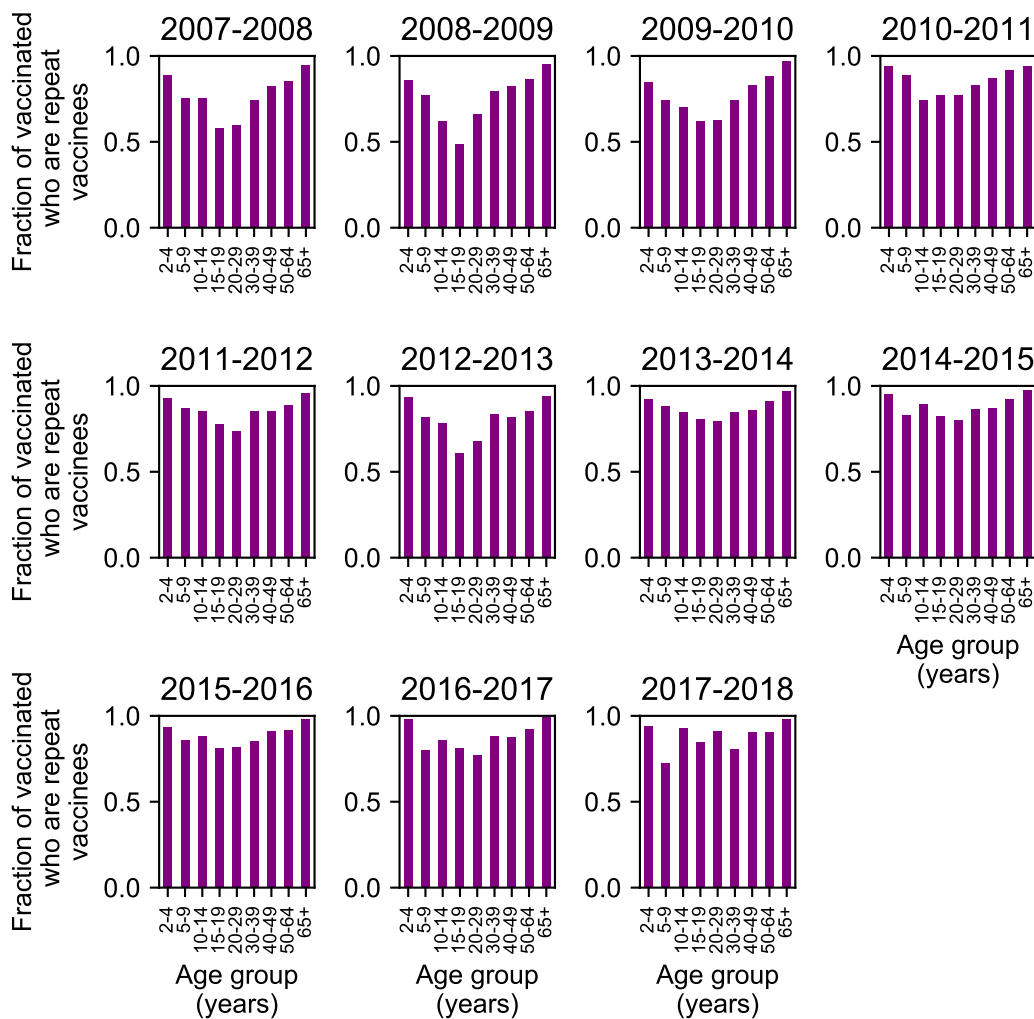


Figure 3–Supplement 3. Repeat vaccination varies by age group and season. Each bar shows the fraction of individuals who were vaccinated in that season who also received at least one influenza vaccination in the previous two seasons.

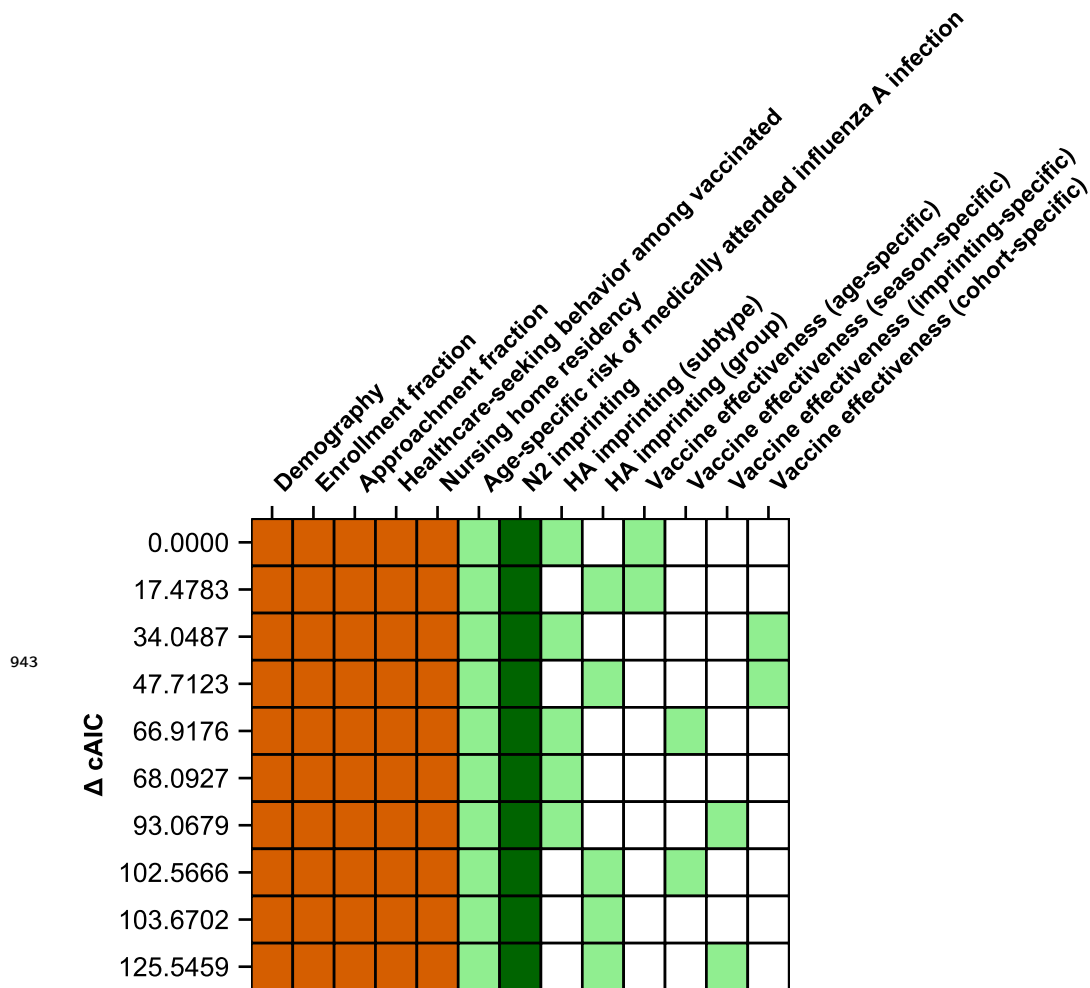
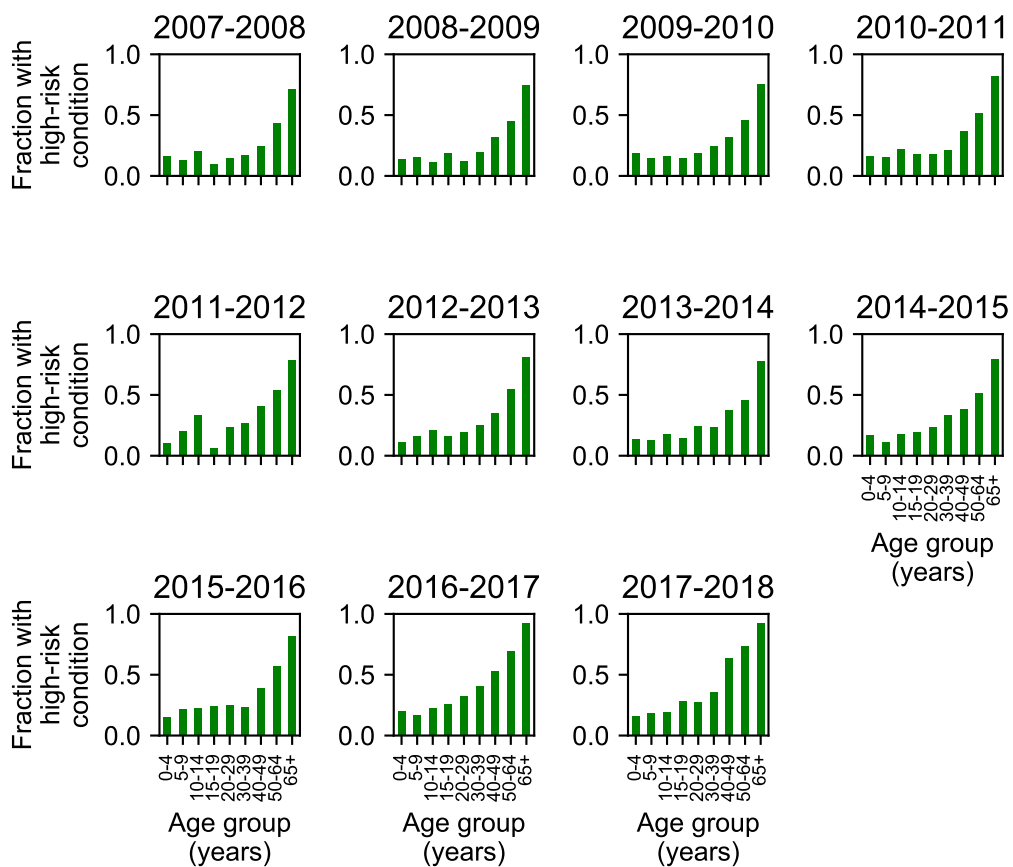


Figure 4–Supplement 1. The best-fitting model includes age-specific risk of medically attended influenza A infection, HA subtype imprinting, and age-specific VE. The ten main models are shown as rows with colored squares indicating whether that model included parameters indicated by the columns. Orange squares indicate covariates that were not estimated. Light green squares mean that a given estimated parameter was supported. Dark green squares mean that the model did not support the inclusion of the parameters indicated by the column (i.e., the CI includes 0). Models are sorted by their cAIC relative to the best-fitting model.



944

Figure 4-Supplement 2. High-risk medical status varies with age but stays relatively consistent across seasons. Each plot shows the fraction of enrolled people who had a high-risk medical condition for each season. High-risk medical condition data was not collected for the 2009 pandemic season.

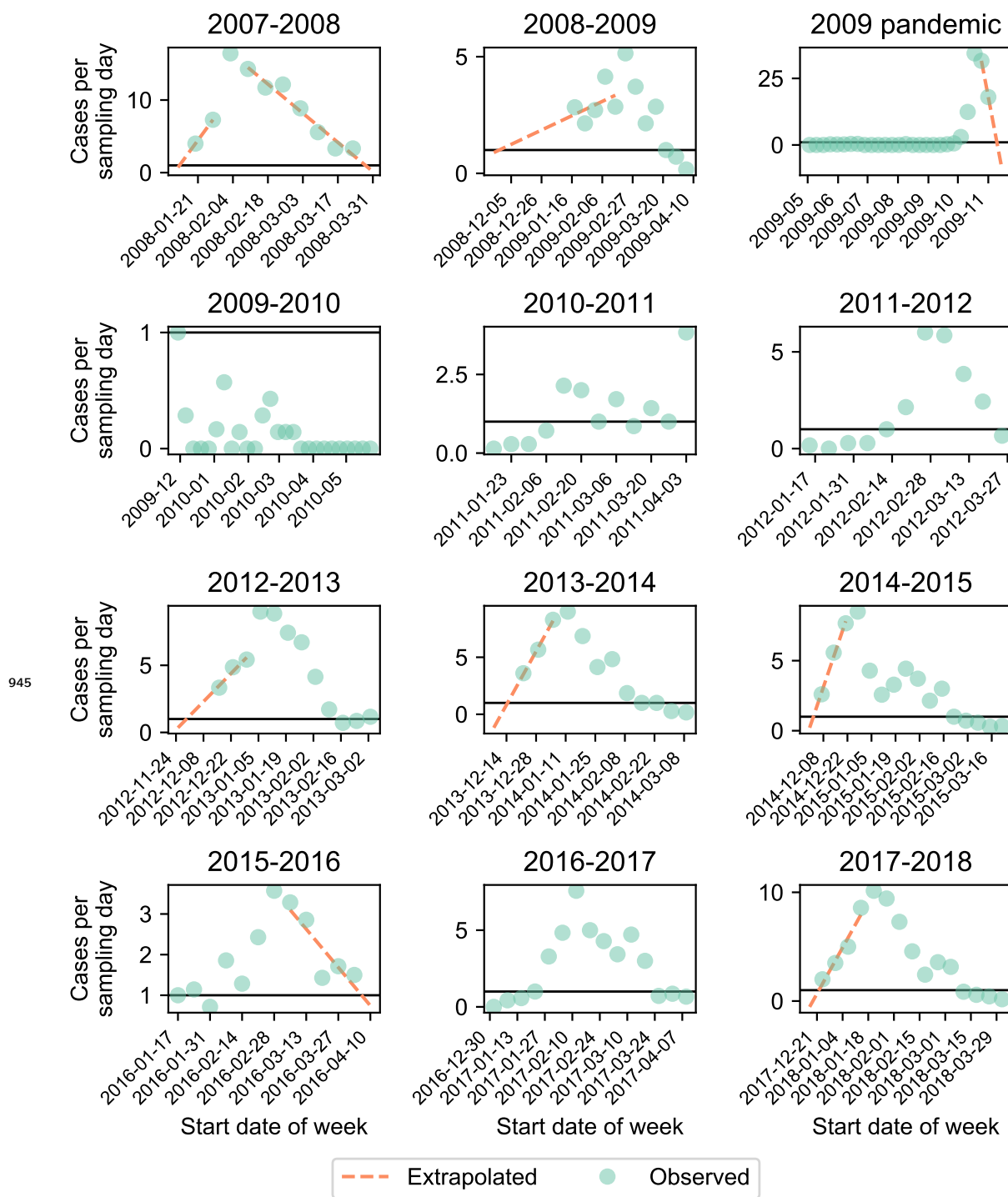


Figure 5-Supplement 1. The starts and ends of some seasons were undersampled. Each panel shows the number of cases per sampling day (green circles). We extrapolated cases at the start and end of the season (orange dashed line) if the observed number of cases per day exceeded 1 (black line) at the start and end of that season (Materials and Methods: "Sensitivity to sampling effort").

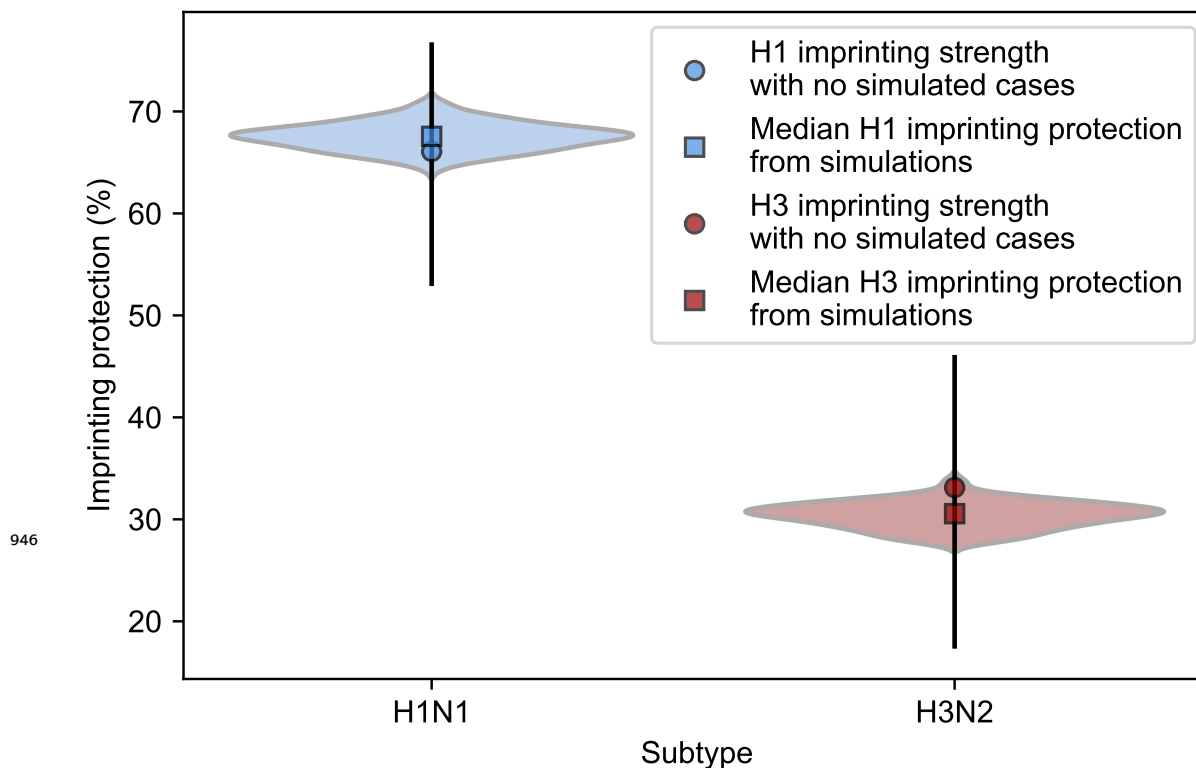


Figure 5–Supplement 2. The strength of imprinting protection does not change significantly after correction for unequal sampling between seasons. We fitted the model to simulated cases in seasons where the enrollment period does not fully overlap the epidemic period and recorded the maximum likelihood estimates for H1N1 and H3N2 imprinting protection (Materials and Methods: "Sensitivity to sampling effort"). The distributions of these values are shown as violin plots and the medians are shown as squares. Estimates of imprinting protection from the best fitting model without simulated data with a 95% confidence interval are shown as circles with error bars.

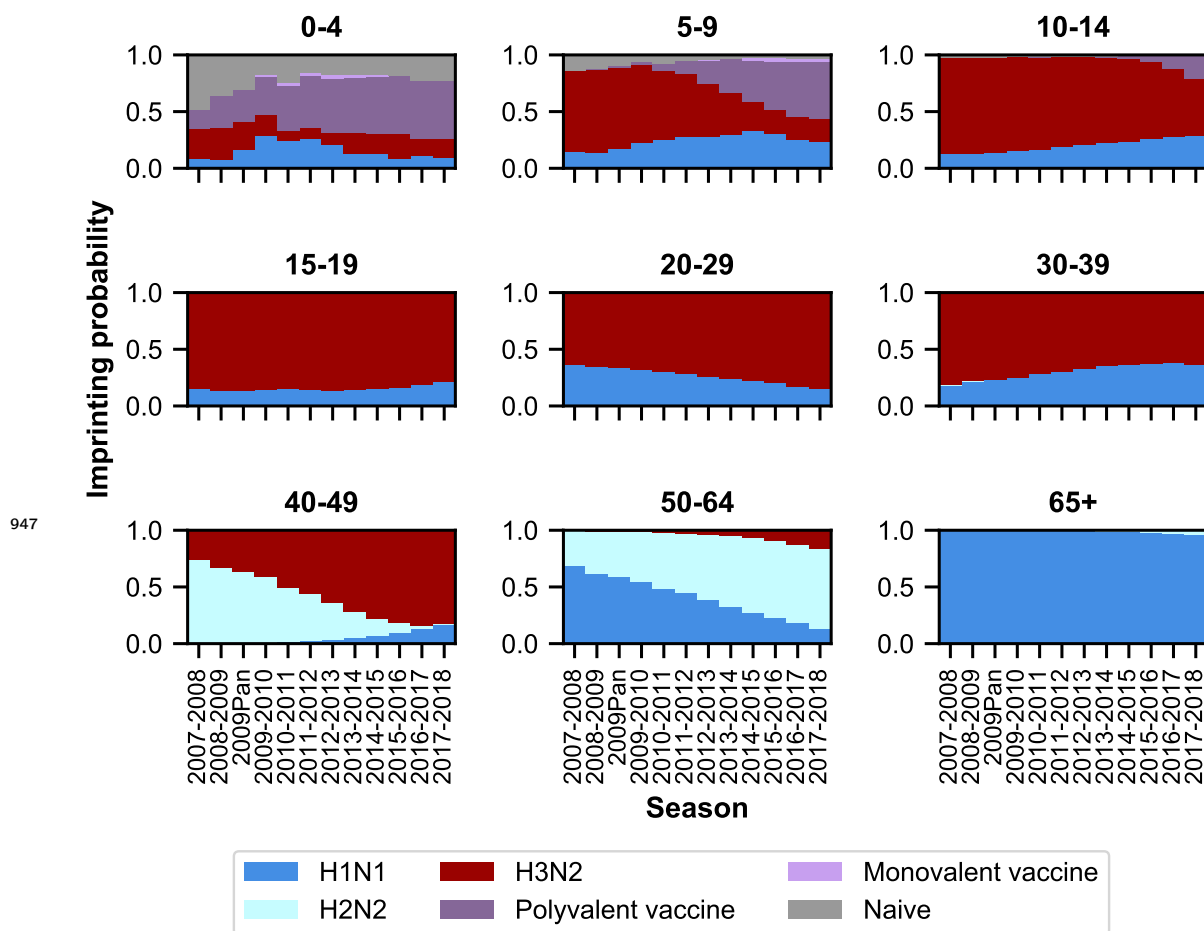


Figure 5–Supplement 3. Each panel shows the imprinting probabilities for a specific age group from the 2007-2008 season through the 2017-2018 season, including vaccination as a potential first exposure.

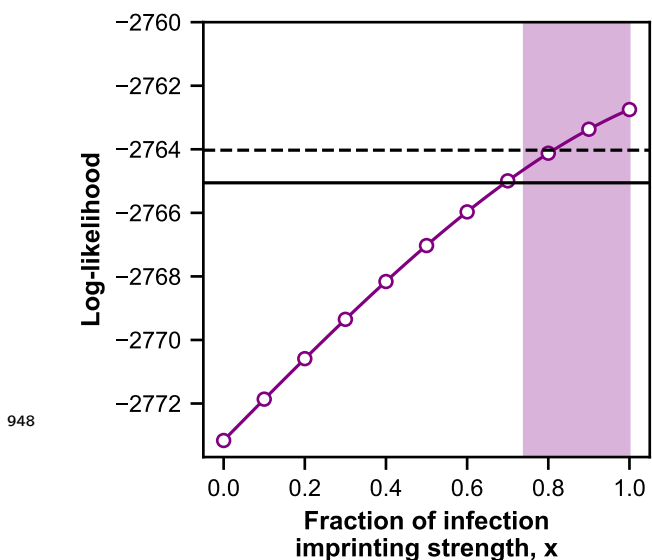


Figure 5–Supplement 4. Vaccine imprinting improves model fit. Plot shows the likelihood profile of the parameter x , which describes the strength of protection from initial exposure via vaccination as a fraction of the protection conferred by initial infection (Materials and Methods: "Vaccine imprinting"). The solid black line shows the log-likelihood of the best-fitting model without protection from vaccine imprinting, and the dashed line shows the log-likelihood threshold for a ΔcAIC of 0 compared to the best fitting model with the addition of one free parameter (i.e., x). Shaded area shows 95% CI for x .

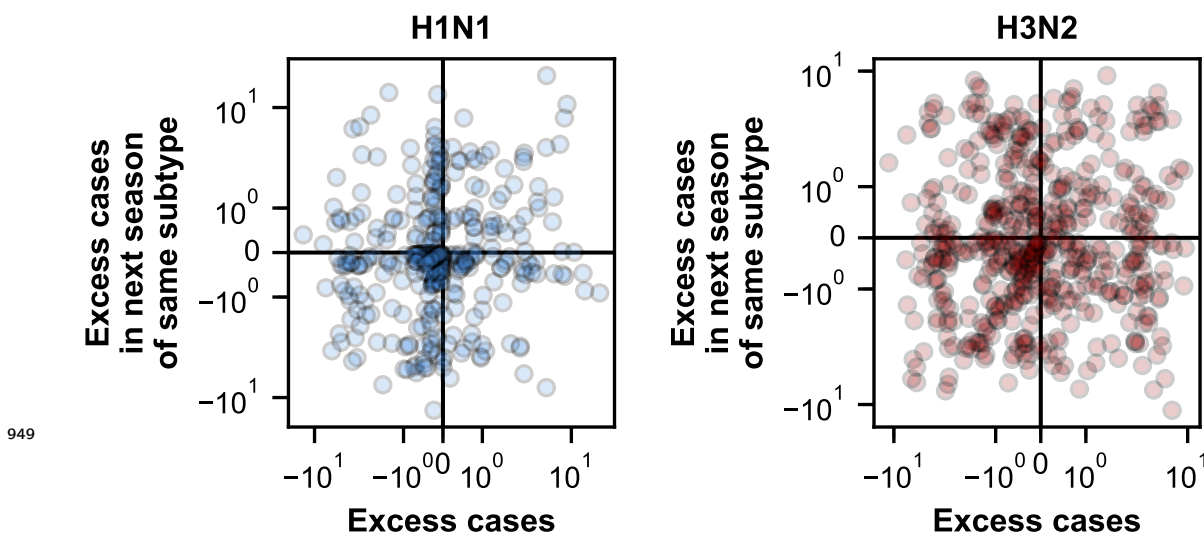


Figure 5–Supplement 5. Excess cases in a season are weakly correlated with excess cases in the next season with the same dominant subtype. We tested whether excess cases in each birth cohort were negatively correlated with excess cases in the same birth cohort in the next season of the same subtype (Materials and Methods: "Calculating excess cases"). If the protective effects of recent infection are not captured in our model, we expect that an excess of cases in one season should lead to a depletion in cases in the next season (i.e., negative correlation). We instead find a weak positive correlation for cases of H1N1 (Spearman's $\rho=0.12$, $p=0.02$) and H3N2 (Spearman's $\rho=0.05$, $p=0.19$).

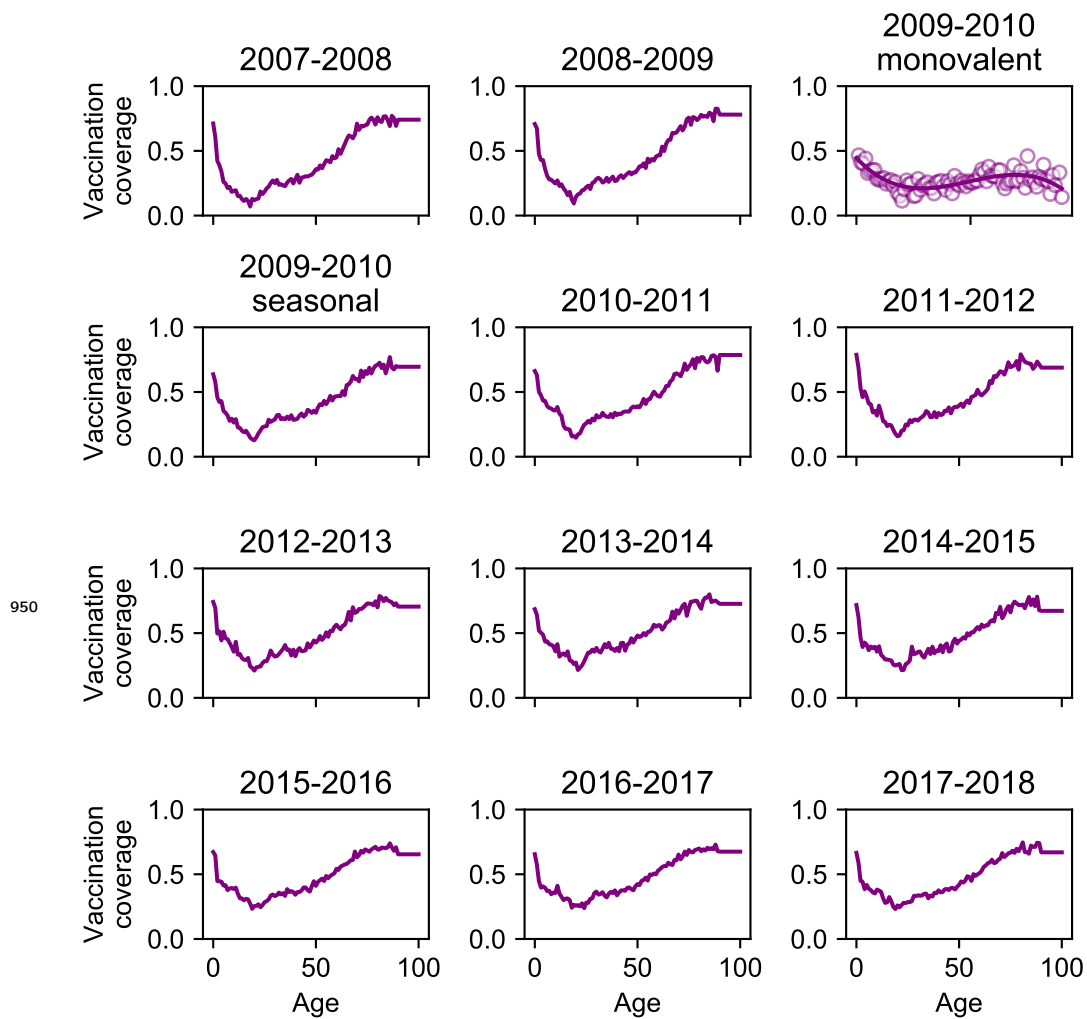


Figure 5–Supplement 6. Vaccination coverage in the Marshfield Epidemiological Study Area for seasons 2007-2008 through 2017-2018. We estimated monovalent vaccination coverage in 2009-2010 by measuring vaccination coverage among enrolled people and fitting a smoothing spline to the data (solid line).

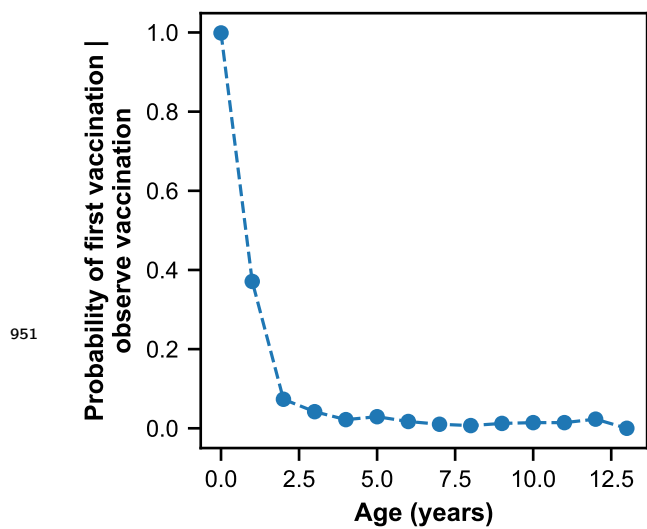


Figure 5–Supplement 7. The probability of an individual receiving their first vaccination declines with age. Each point represents the fraction of people enrolled in the Marshfield study who received their first vaccination among all vaccinated individuals of that age.

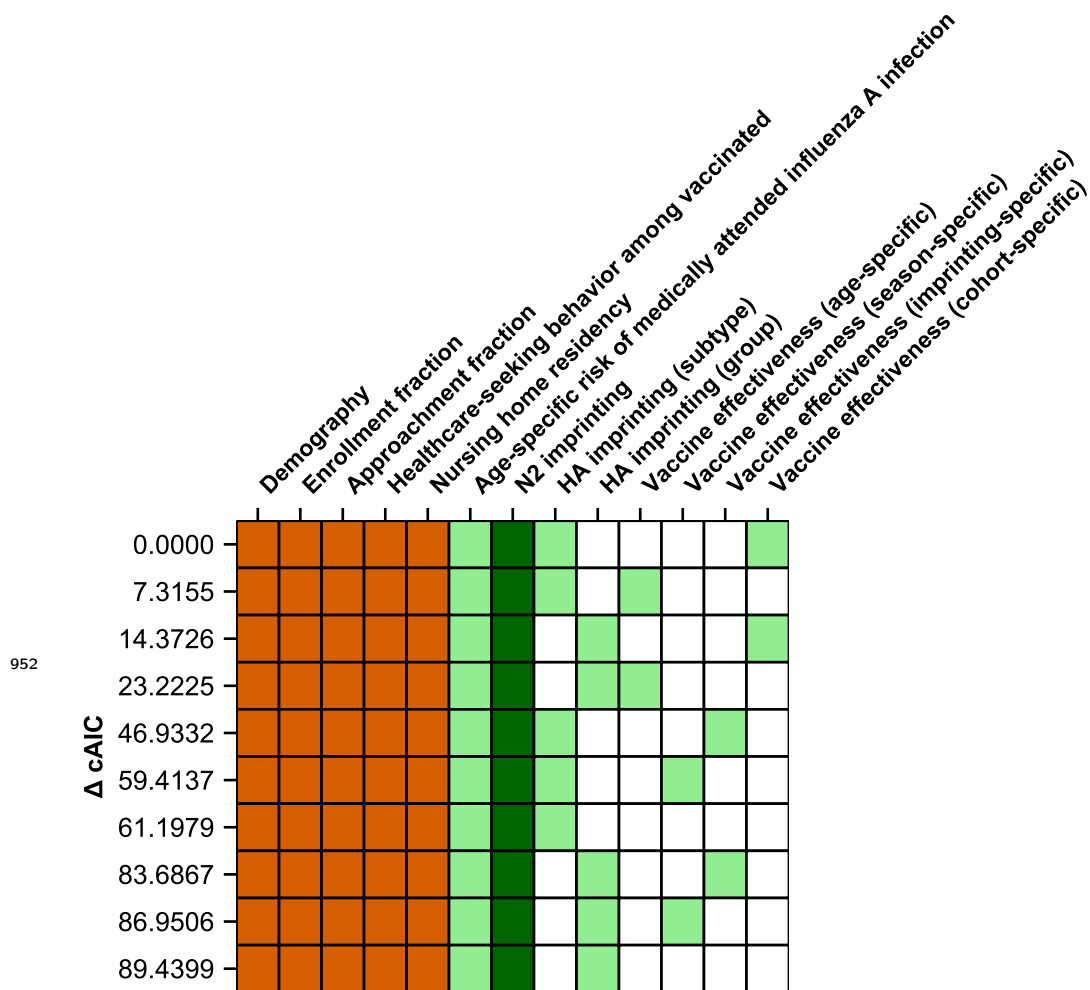


Figure 6–Supplement 1. A model including age-specific risk of medically attended influenza A infection, HA subtype imprinting, and birth-cohort-specific VE best fits cases of people ≥ 10 years old. The ten main models are shown as rows with colored squares indicating whether that model uses parameters indicated by the columns. Orange squares indicate covariates that were not estimated. Light green squares mean that a given estimated parameter was supported. Dark green squares mean that the model did not support the inclusion of the parameters indicated by the column (i.e., the CI includes 0). Models are sorted by their cAIC relative to the best-fitting model.

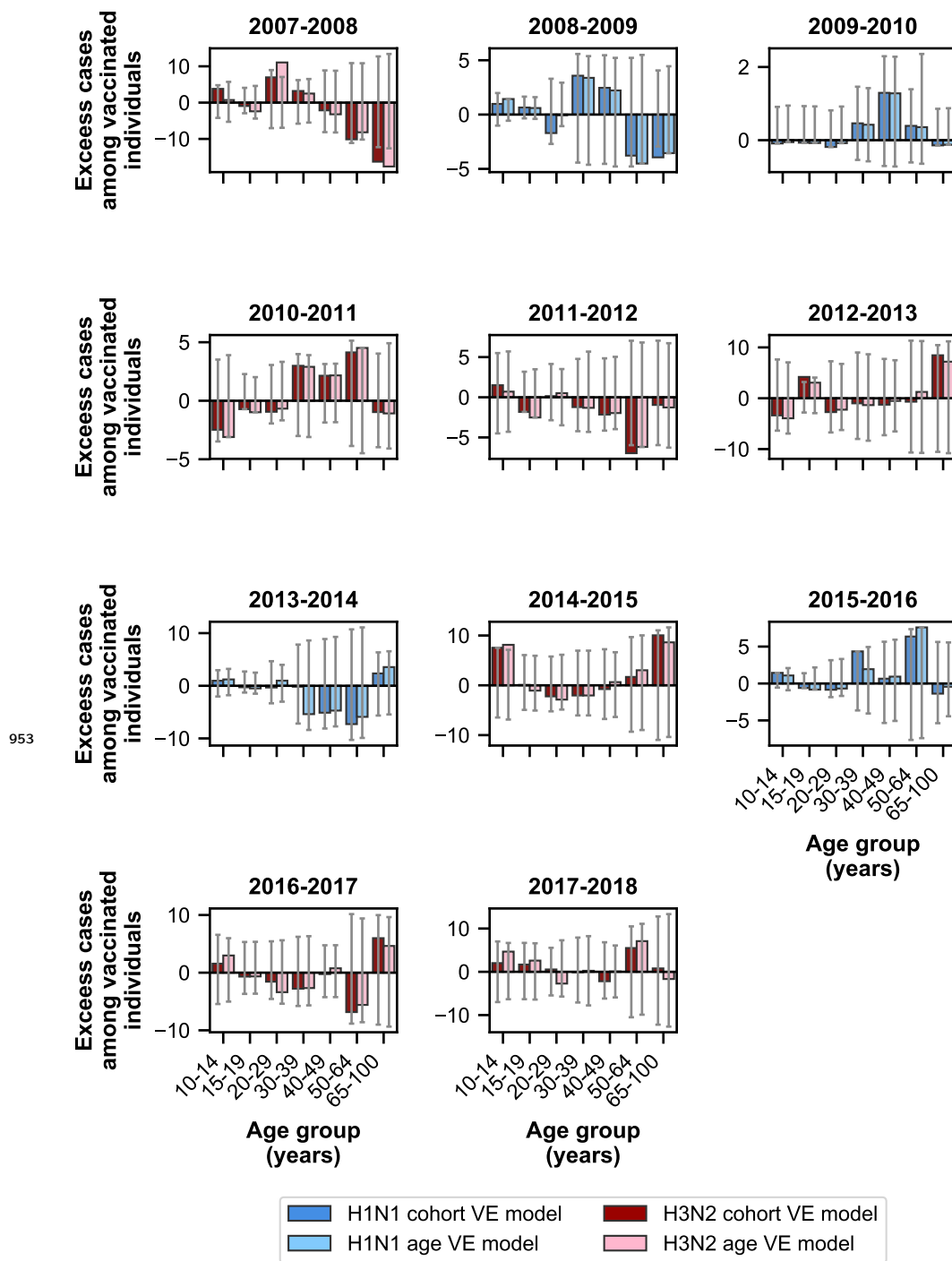


Figure 6-Supplement 2. The birth-cohort-specific VE model predicts observed cases better than the age-specific VE model for people ≥ 10 years old. Bars show the excess cases in vaccinated individuals relative to the birth-cohort-specific VE model (dark colors) and the age-specific VE model (light colors) for age groups ≥ 10 years old. Colors indicate the dominant subtype of a given season. 95% prediction intervals are shown as grey error bars.